PAP-729

Hydraulic Model Study of Spillway Modifications and Dam Overtopping for Coolidge Dam, Arizona

by

Perry L. Johnson

May 1996

PURPOSE AND APPLICATION

Hydraulic model studies were conducted to evaluate and refine hydraulic features associated with the rehabilitation of the spillways and passage of the probable maximum flood (PMF) by dam overtopping at Coolidge Dam, Arizona. Of particular interest was evaluation of impact pressures and flow velocities on abutment and downstream rock surfaces during overtopping. In addition, the discharge capacities of the spillways were rated both with and without gate control with the existing crest profile and with the proposed modified profile. The cavitation potential on the chutes was evaluated using a computer model, and aeration ramps were designed using a computer model and the physical model. Finally, both balanced and unbalanced gate operation were evaluated with best and worst operating conditions noted. Overtopping ratings were developed and local tailwater levels around the toe of the dam determined. The potential for erosion on the abutments and at the dam toe was also investigated.

The results of this study have only limited application at other sites. Many of the flow features observed are strongly dependent on structure and topography configuration. Consequently, the study results tend to be very site-specific. The findings may give general insight which would aid work at other hydraulic structures.

INTRODUCTION

Coolidge Dam (figs. 1 and 2) is owned and operated by the Bureau of Indian Affairs (BIA) and is located on the Gila River in southeast Arizona in the eastern portion of Pinal County about 30 miles southeast of Globe, Arizona. Construction of the dam was authorized on June 7, 1924, and completed in November 1928. The dam is a multiple dome, reinforced concrete structure designed by the BIA. There are three domes which are supported by massive buttresses on 180-ft centers. The hydraulic height is about 220 ft above streambed with a crest length of about 920 ft including the spillways. The dam crest serves as a roadway that is 20 ft wide. The 166-ft-wide gated chute spillways are located on each abutment. Each spillway crest includes three 50- by 12-ft drum gates which became inoperable (in the down position) shortly after completion of the dam. Downstream of the crest, each spillway narrows to a 60-ft-wide superelevated chute. The chutes release the flow directly into the river with no stilling basins. Reservoir capacity at the spillway crest, elevation 2510.6, is about 910,000 acre-feet. Irrigation and hydropower releases are controlled from a powerhouse located beneath the center dome.

Safety of dams studies, which included consideration of an updated PMF, found the failure potential of the dam to be high because of the inability of the spillways to pass the PMF. Flood routings showed that the maximum releases from Coolidge Dam would be 459,000 ft^3/s. Combined safe spillway capacity was thought to be about 80,000 ft^3/s. To safely pass the PMF, several modifications were considered including realigning and replacing the spillways and allowing dam overtopping while providing erosion protection to downstream rock surfaces. The overtopping option with a limited rehabilitation of the spillway structures was selected.

CONCLUSIONS

1. The pronounced superelevation in the right chute (looking downstream) combined with the chute convergence and the horizontal and vertical curves yield a standing wave for most operating conditions. The superelevation concentrates the flow and directs it toward the left chute wall causing abrupt flow impingement and fins rising up the wall. With both spillways releasing 50,000 ft^3/s to more than 100,000 ft^3/s, the finning generates splash over the chute wall. At discharges approaching 200,000 ft^3/s and higher, the wall is overtopped, yielding flows with velocities approaching 100 ft/s over abutment surfaces. At discharges below 25,000 ft^3/s with balanced or uniform gate operation, the flow is so concentrated to the left that often much of the right side of the chute is dry.

2. Through use of unbalanced gate operation on the right spillway, the standing wave, finning, and flow distribution on the lower chute can all be improved. Unbalanced gate operation with predominant use of the inside and middle gates is recommended as an operational alternative when combined spillway releases are less than about 40,000 ft^3/s. At discharges above 40,000 ft^3/s, large gate openings are required on all gates.

3. Flow conditions on the left spillway are strongly influenced by the flat gradient of the upper chute and the chute convergence and horizontal curve. Again, a standing wave is generated although wave impingement on the inside chute wall is not as severe as that on the right spillway. Flow in the left chute is well contained for combined spillway releases up to 75,000 ft^3/s . At combined spills of 100,000 ft^3/s and greater, the flow overtops the outside chute wall at about station 2+00. With combined spills of 200,000 ft^3/s or greater, the upper chute has insufficient gradient to carry the flow downstream. As a result, the upper chute fills with water and the upper inside chute wall is overtopped. Again, overtopping will generate flow velocities across topography surfaces approaching 100 ft/s.

4. Unbalanced gate operation can be used to improve flow conditions on the left spillway chute. Predominately using the outside and middle gates provides better approach flow to the lower chute which reduces the standing wave and improves the flow distribution on the lower chute. Balanced operation must be used above 40,000 ft^3/s.

5. Dam overtopping starts at a combined spill of about 150,000 ft^3/s. Initially, overtopping is concentrated at the abutments with overtopping flow intercepted by the spillway chutes. The PMF release of 459,000 ft^3/s can be passed with a reservoir elevation of 2555.6, assuming gate and parapet failure, or with a reservoir elevation of 2557.5 with parapet and gate influence.

6. Impact pressures on downstream topography resulting from dam overtopping are greatly reduced by tailwater effects. However, with shallow or no submergence of topography, the full vertical drop from the reservoir water surface to the topography can be developed as an impact pressure. Limited model data show that, at a discharge of 380,000 ft^3/s with submergence of 69 to 81 ft, dynamic pressures on the topography surface at the dam toe range from 15 ft above the tailwater generated hydrostatic pressure to 7.5 ft below, resulting in local uplift pressures.

7. Tailwater elevations at the base of the dam are strongly influenced by the hydraulics of the flow exiting the spillway chutes, particularly for combined spills of less than 250,000 ft^3/s. Flow exiting from the spillway chutes tends to sweep downstream reducing tailwater elevations between the spillway chutes and the dam. Potentially, tailwater elevations can be reduced by 20 to 30 ft (below levels predicted in the tailwater analysis) for discharges ranging from 50,000 ft^3/s to 200,000 ft^3/s. As scour holes develop, tailwater reductions caused by spillway flow will be reduced. Likewise, tailwater reductions caused by spillway flow are less significant at high discharges with heavy overtopping.

8. A computer model cavitation analysis of the spillway chutes shows that flow with velocities in excess of 100 ft/s can cause significant cavitation damage unless small surface tolerances can be maintained (no abrupt offsets greater than 0.25 in and no chamfers steeper than 1 on 19). It would seem unlikely that flow surfaces of this quality will be maintained over the life of the structure. Thus, it would be prudent to aerate chute flows to control potential cavitation. Aeration structures, which include floor and side wall ramps, are recommended. The ramp construction would minimize cost. The computer model indicates that the ramp design will supply more than sufficient aeration. Physical model observations show the design to be workable.

9. The dam abutments will be protected with reinforced concrete mats where necessary. The left abutment will be stabilized with a concrete buttress wall. The toe of the dam will be protected by placing 3 ft^3 quarry stones weighing between 2000-4000 lbs in the overtopping impact area.

THE MODEL

The hydraulic model (fig. 3) of Coolidge Dam was constructed at a Froude scale of 1:55. Included in the model was a detailed representation of the entire dam including spillways, outlet works, powerplant intake towers, parapet walls, and roadway bridges over the spillway crests. Care was taken in representing structural details because of their influence on the overtopping rating and overtopping characteristics. Also included in the model were a 380- by 1,150-ft area of reservoir topography and a 770- by 940-ft area of tailwater topography. Sufficient topography was included to correctly represent approach flow conditions in the reservoir and tailwater flow patterns, including flow-influenced tailwater elevations. Topography was modeled with a rigid surface; consequently, scour that would occur below the spillways was not modeled. This scour would influence tailrace flow patterns, in particular, at low and intermediate discharges. Under overtopping discharges, tailwater depths become substantial and supply an energy dissipation pool. Tailwater depths were set based on a topography controlled tailwater analysis done by the Sedimentation and River Hydraulics Group (formerly Sedimentation Section, Surface Water Branch) [1].

During initial testing, the flow distribution entering the model was evaluated and adjusted. Reservoir water surface elevation and tailwater elevation gages were set. Available drawings and data on the structure were limited and at times conflicting. Field surveys were taken to

better define upper spillway surfaces. Also, a field visit to the dam allowed examination of structure details that were poorly defined on drawings. After the field visit, a few model details were adjusted. At this point it was felt that the model was representative and would yield true flow representation. As one check, the model was operated at a discharge of 3,000 ft^3/s, which corresponded to a prototype spill which had been photographed. Flow patterns on the chute, including standing wave positions and sections of the right spillway chute over which there was no flow, were correctly represented.

Discharges to the model were set using the laboratory venturi meters. Velocities in the model were measured using propeller meters and video tape of surface floats when the flow was shallow and heavily aerated. Dynamic impact pressures were measured using a flush-mounted pressure transducer. Static impact pressures were measured with piezometer taps and a manometer board. Limited impact pressure data were taken in the model. Data taken were used to confirm theoretical predictions that consider jet breakup and air entrainment.

THE INVESTIGATION

General Flow Features - Initially, both spillway controlled and dam overtopping discharges were rated with the existing crest configuration and with no gate control. These tests defined the performance characteristics of the existing structure. As the structure was rated, general flow patterns were observed. Spillway flow conditions were always documented with combined discharge totals for both spillways operating, unless otherwise noted. The flow patterns on the two spillways were significantly different because of differences in the chute geometries (fig. 4).

The right spillway (looking downstream) includes pronounced superelevation which begins immediately downstream of the crest section. This superelevation, combined with the chute convergence and horizontal and vertical bends, leads to the 60-ft-wide lower chute with a slope of about 0.4.

The left spillway includes much less superelevation and has an extended low gradient chute immediately downstream of the crest section. The chute converges, combined with horizontal and vertical bends, leading to a 60-ft-wide chute with a slope of about 0.73.

Right spillway flow conditions - Flow conditions on the right spillway are strongly influenced by the superelevation and horizontal and vertical curves in the upper chute. With combined spillway discharges less than 10,000 ft^3/s, the superelevation on the right spillway generated a standing wave and concentrated and directed the flow to the left side of the chute with much of the right side of the chute dry. As a result, the flow impinged on the left chute wall at about station 3+80 where it climbed the wall forming a fin. With a release of 10,000 ft^3/s, the fin reached about the top of the wall, but no overtopping of the wall was noted. As the flow passed on down the right chute, it spread to the full chute width near the bottom.

With a combined spill of 25,000 ft^3/s, the top of the fin was above the top of the left wall; however, no overtopping occurred. At 25,000 ft^3/s, the flow overrode the superelevation such that all of the chute had some flow covering it; however, the flow was shallow near the right spillway wall. With a combined spill of 50,000 ft^3/s, the fin extended well above the wall and some splash over the left wall occurred downstream from the standing wave impact point.

At 75,000 ft^3/s, the upper portion of the chute, immediately downstream from the crest and piers, was nearly full of water to the top of the chute walls. The standing wave, generated by the superelevation and horizontal bend, advanced up to nearly the downstream end of the right crest pier (fig. 5). The fin generated by the impingement of the standing wave extended well above the wall and generated significant splash over the wall. The tailwater had risen onto the lower walls of the chute.

At a combined spill of 100,000 ft^3/s, fin generated splash over the wall continued to increase and the standing wave advanced up to the downstream end of the right crest pier. At 200,000 ft^3/s, weak overtopping of the dam occurred which included overtopping of the roadway bridges on the spillway crest. The nose of the wave advanced up under the bridge and impinged high on and partially overtopped the left chute wall. Both the overtopping of the chute wall and the overtopping of the dam yielded flow over the ground surface between the chute and the right dome of the dam.

At 300,000 ft^3/s, the flow patterns described for 200,000 ft^3/s continued, except both dam overtopping and chute wall overtopping flows were heavier. The nappe of the bridge overtopping flow was well aerated and an air cavity was present behind and below the bridge.

Finally, at the PMF spill of 459,000 ft^3/s, the flow conditions were heavier yet. The zone below and downstream of the bridge was only partially vented. The tailwater was well up onto the chute which yielded a plunging supported jet into the tailwater pool.

Left spillway flow conditions - Flow patterns on the left spillway are strongly influenced by the flat gradient of the upper chute and secondarily influenced by the horizontal and vertical curves. With total spills of 75,000 ft^3/s and less, the flow distribution below the crest was fairly uniform. A standing wave occurred on a diagonal across the chute (fig. 6); however, its impingement on the right chute wall was not as severe as that on the left wall of the right spillway. Flow distribution on the lower chute tended to be fairly uniform.

The position of the standing wave advanced upstream toward the piers and crest with increasing discharge. At 75,000 ft^3/s, the standing wave approached the left crest pier and the upper chute was nearly full of water. With a total spill of 100,000 ft^3/s, the nose of the standing wave advanced to the piers and the flow filled the upper chute to the top of the walls and overtopped the lower left chute wall at about station 2+00.

At 200,000 ft^3/s, the nose of the standing wave was above the downstream end of the piers under the bridge. Because of the flat gradient of the upper chute, the chute could not contain the flow. The flow overtopped the right chute wall producing flow across the ground surface between the left spillway chute and the left dome of the dam. In addition, shallow overtopping of the dam and the roadway bridge occurred (fig. 7a). The overtopping yielded additional flow across the ground surfaces. The nappe of the flow overtopping the bridge was well aerated.

At 300,000 ft^3/s, the wave had advanced further up under the bridge and both dam and chute wall overtopping flows were heavier. The nappe of the bridge overtopping flow continued to be adequately vented.

Finally, at 459,000 ft^3/s, deeper overtopping flows were observed and the bridge overtopping flow was only partially vented (fig 7b). Tailwater elevations increased greatly with discharge yielding substantial submergence of the lower chute at the PMF.

Dam overtopping flow conditions - As the reservoir water surface rises to the top of the roadway at elevation 2535, overtopping begins (fig. 7). The parapets supply substantial overtopping blockage, preventing substantial overtopping until the reservoir rises above the top of the parapets at elevation 2540. It was recognized that the parapets may fail, in particular under larger overtopping flows. Therefore, overtopping flows were studied both with and without the parapets. Initially, the heaviest overtopping occurred over the roadway surface approaching the dam. These overtopping flows were either intercepted by the spillway chutes or passed down the roadway over the dam and through the downstream parapet. Over the full overtopping discharge range, horizontal velocity components were small compared to velocities generated by the vertical fall. Therefore, dam overtopping flows dropped nearly vertically to the tailwater or ground surface below the dam. No direct flow impingement on the powerhouse occurred.

Discharge Ratings - The existing spillways with no gate control were rated because the gates are currently inoperable and in the down position. Figure 8 is a discharge rating for both spillways operating in combination. Figure 9 is a discharge rating for the right spillway, and figure 10 is a discharge rating for the left spillway. A discharge of about 150,000 ft^3/s can be passed prior to overtopping. Figure 11 shows overtopping ratings both with and without the parapets. Note that with parapets the PMF is passed with the reservoir at elevation 2557.5 and without the parapets the PMF is passed with the reservoir at elevation 2555.6 or 1.9 ft lower. The overtopping dam passes a discharge of about 309,000 ft^3/s in addition to the spillway flows. Finally, figure 12 presents the total combined rating curve for the existing structure with uncontrolled spillways and the roadway parapets on top of the dam.

To upgrade the structure, it is proposed to replace the drum gates with radial gates and a modified crest profile. To provide sufficient vertical wall surface to seat the radial gates against and to support the gate hoist deck, the crest piers and spillway sidewalls will be extended upstream (figure 13). The crest profile was modified to improve its efficiency and the crest elevation was raised 0.4 ft above the elevation of the existing crests to elevation 2511.0. The modified crest structures, both with and without gate influence, were then rated. Figure 14

shows the developed rating for an uncontrolled crest and for operation with balanced or uniform gate control. The PMF is passed with an additional 0.5 ft increase in reservoir elevation when compared to the existing condition with parapets on the roadway. The higher reservoir elevation is caused by the influence of the gates and the hoist deck during overtopping.

Tailwater Elevations - Tailwater elevations in the model were set based upon the computed tailwater elevations at station 2 of the tailwater analysis [1]. Station 2, located about 600 ft downstream from the dam, was selected because it was far enough downstream of the dam and spillways that flow patterns are controlled by canyon topography and not structure influence.

Shown in figure 15 are the tailwater elevations developed by the tailwater analysis for stations 1 and 2. The analytical backwater curves show an increase in the tailwater near the dam. Tailwater elevations at station 1, immediately downstream from the powerhouse are, however, influenced by the spillway flows. In the model, with no scour hole development below the chutes, the flow exiting the spillway chutes sweeps downstream depressing the tailwater between the spillways and the powerhouse. This effect is most pronounced for discharges of about 200,000 ft^3/s or less.

Using the appropriate tailwater was vital to determining flow conditions in the river channel and at the toe of the dam. The tailwater pool becomes deeper at higher discharges and the sweeping influence is reduced. Figure 15 also shows the tailwater elevation observed at station 1 in the physical model. Note that the sweeping action of the spillway depresses the tailwater at the powerhouse, in particular for discharges from 100,000 to 200,000 ft^3/s. The net effect is the reduction of maximum tailwater elevations at the powerhouse of up to 30 ft. It should be cautioned that as scour holes develop, the flow exiting the chutes may be either redirected or considerable velocity may be lost. Either or both of these factors can reduce the sweeping action and generate tailwater elevations at the powerhouse that are nearer to those predicted by the initial analysis.

Flow Velocities - Flow velocities were evaluated in the model by video taping surface floats and using propeller meters. Video taping of surface floats was used in many places because the broken flow and heavy air entrainment characteristics did not allow more conventional metering. Results from the video technique were, in places, influenced by the angle of the camera distorting measurement of travel distances and affecting the computed velocities. Flow velocities on the chutes were also evaluated using a computer model as part of a cavitation analysis. The findings of these studies are summarized in figures 16, 17, and 18.

Figure 16 shows observed flow velocities with a total release of 80,000 ft^3/s. The low tailwater at this discharge yields maximum surface to tailwater head differentials which will yield maximum velocities in the river channel. Scour holes were not included in the model; therefore, limited energy dissipation occurs as the flow exits the chutes. The rock surface downstream of the chutes will be exposed to the maximum velocities shown in figure 16. The video indicates maximum velocities of up to 130 ft/s. This exceeds the 118 ft/s produced by the available head and the 103 ft/s maximum velocities that the computer analysis indicates. However, using the

video-evaluated velocities for design will give representative, although conservative, results. Velocities between the flows exiting the chutes and the powerhouse tend to be low with velocities at the powerhouse near zero.

Figure 17 shows observed flow velocities with a total release of 300,000 ft^3/s. The velocities at the lower end of the chutes approach 110 ft/s which corresponds closely to the computer model prediction. The flow velocities of 90 to 100 ft/s over topography surfaces are theoretically possible. This flow is highly broken and aerated and thus cavitation erosion on these surfaces is unlikely. Shown are observed overtopping velocities of 14 to 18 ft/s that the roadway and upper abutment surfaces must withstand. Also shown is the approximate impact position of the overtopping jet. Although flow velocities over the topography surfaces behind the jet (inside the domes) were not measured, the jet was split and flow conditions were observed. Very little hydraulic action occurs except in the vicinity of the impact.

Figure 18 shows observed flow velocities with a total release of 459,000 ft^3/s. The flow velocities in the chutes, over the topography, and overtopping were about the same as observed at 300,000 ft^3/s. At these high discharges, in particular on the right abutment, the high tailwater levels greatly reduced the area of free flow over the topography surface making measurements difficult.

Overtopping Impact Pressures - Impact pressures at the dam toe were evaluated by using an impingement theory developed by Ervine and Falvey [2] and model measurements. Model results produce conservative impact pressures from overtopping jet impingement primarily due to scale effects which reduce model jet breakup and air entrainment. The theory was used to evaluate mean impact heads, and with a lesser degree of accuracy, maximum dynamic impact heads, as a function of discharge and tailwater depth. The theory was developed for a compact or circular cross-sectional jet geometry. It considers factors including initial jet thickness and velocity (critical depth) at the top of the dam, initial jet turbulence levels and air entrainment, the vertical fall to the ground or tailwater surface, and the tailwater depth.

The jet breakup and air entrainment are determined for the free falling jet from the initial cross section and flow properties. The characteristics of the jet at the tailwater surface are defined and jet diffusion as a function of depth in the tailwater pool is evaluated. This yields jet velocities as a function of depth and resulting mean dynamic impact pressures. Impact heads were computed based on a gravity corrected jet diameter and on 80 percent of the computed outer limit of the diffused free jet at the tailwater surface. The tailwater measured in the model at the toe of the dam (station 1 hydraulic model, fig. 15) was used for a conservative representation in this analysis.

Ervine and Falvey note that computed mean impact heads are approximate. They note that maximum dynamic heads might be related to "almost" the outer edge diameter of the jet at the tailwater surface, which for this analysis was assumed to be 80 percent of the spread jet diameter (with a turbulence intensity of 4-5 percent which would yield an outer jet spread of about 3 percent). Results of the analysis are summarized in Table 1.

Table 1. - Computed impact heads as a function of discharge and tailwater.

Total release (ft^3/s)	Reservoir elevation	Tailwater elevation (observed at dam)	Local tailwater depth (ft)	Local impact head (ft)	
				Mean	Estimated maximum
200,000	2542.6	2354.5	25	0.30	188
			50	0.07	81
			75	0.03	34
300,000	2548.8	2382.0	25	2.71	167
			50	0.68	61
			75	0.30	27
			100	0.17	15
400,000	2554.1	2405.0	25	8.29	149
			50	2.07	48
			75	0.92	22
			100	0.52	12
			125	0.33	8
459,000	2557.0	2427.0	25	13.10	130
			50	3.28	36
			75	1.46	16
			100	0.82	9
			125	0.53	6
			150	0.36	4

This analysis shows that even at the maximum discharge, the mean impact pressures are small indicating that the overtopping jet is thin. The jet will break up as it falls with the resulting core at the tailwater surface being nonexistent to very thin. The thin jet core and the heavy air entrainment causes the jet to quickly disperse in the tailwater pool resulting in generally low mean impact heads. The tailwater significantly influences the mean and dynamic impact heads. The analysis shows that at a discharge of 459,000 ft^3/s, the mean impact head is 13.1 ft of water with a tailwater of 25 ft and only 0.36 ft with 150 ft of tailwater. The analysis indicates, however, that maximum dynamic impacts may be substantially greater.

Ervine and Falvey caution that little research has been accomplished to define dynamic maxima and thus, this analysis is at best speculative. Note that the analysis shows that for a particular tailwater depth, i.e. 50 ft, greater dynamic heads can be developed at the smaller discharges. Even though the vertical drop from reservoir water surface to tailwater surface is greater at

200,000 ft^3/s, it seems that energy dissipation with the thinner jet would be substantial and that this increase in impact heads would be questionable. For the shallow tailwater depth of 25 ft, the tailwater is shallower than the zone of flow establishment and full reservoir impact head is predicted to develop.

To confirm the theory, direct measurements of impact heads with tailwater influences were made in the model. The Froude scale physical model should overestimate impact heads. Impact heads measured in the model should be greater than both the computed impact heads shown in Table 1 and the actual impact heads that will occur at the prototype structure.

Data were collected at a single point from a piezometer tap and manometer used to measure static head and a flush-mounted transducer used to measure dynamic heads. These data were used to confirm the theoretical computations and to evaluate potential dynamic fluctuations, and not to define the full impact pressure field. Visually, attempts were made to position the piezometer and transducer so that maximum jet impingement would occur on them at the maximum discharge of 459,000 ft^3/s.

After installation, it was observed that the maximum impact occurred at a discharge of about 380,000 ft^3/s. Consequently, all data were collected at that discharge. To maximize measured impact pressures, the tailwater was set as low as possible with the tailwater surface elevation varying between 2365 and 2377. The piezometers and transducer were mounted at elevation 2296 which yielded 69 to 81 ft of submergence. Mean measured impact heads were about 3.7 ft of water. Measured maximum dynamic fluctuations indicated that heads could vary from 15 ft above the tailwater to 7.5 ft below, which could produce uplift. Comparing these measured values to the computed values for 400,000 ft^3/s and 75 ft of tailwater, indicating a mean of 0.9 ft with dynamic fluctuations of 22 ft, it appears that the computed values are reasonable.

Finally, figure 19 shows the observed zone over which direct impact by the overtopping flow occurred. This can be coupled with the tailwater curve (fig. 15) and with the theory (Table 1) to define the total impact pressure field that may be encountered at various locations at the toe of the dam and on the abutments.

Dam Overtopping Protection - Concern about the rock quality and high impact pressures on the dam abutments and toe led to further investigation of necessary overtopping protection. The dam will overtop for flows from 150,000 to 459,000 ft^3/s with a maximum overtopping head of 22.5 ft. The abutments and toe of the dam will experience impact from the overtopping flows. The areal extent of the overtopping impacts were documented by the model (fig. 20). The spillway walls were overtopped which produced concern for abutment erosion before the dam began overtopping. Flows over the abutments increased with discharge passed by the dam. The design team determined that abutment stability must be assured and designed concrete protection for all areas indicated by the model. A concrete thickness of 2.5 ft, measured perpendicular to the slope face, has been designed to protect the abutments. Limits of the overtopping protection extends 250 ft and 320 ft downstream of the dam on the right and left abutments, respectively,

and is located between the downslope side of the chutes and elevation 2340.0. On the left abutment, a large buttress wall covers the cliff area near the base of the dam. Two other areas will be covered with overtopping protection on the left abutment. One of these areas is the ridge just downslope of the right chute wall, and the other will be a strip of area 15 ft wide just upslope of the left chute wall. On the right abutment, an additional measure of overtopping protection is provided upslope of the right chute wall, and for the dam access road. The end of both spillways will be protected with an end sill, with a key extending 5 ft into the rock. Drainage will be provided for the entire area. The large cliff area at the left abutment will be protected by a concrete buttress wall.

These features were constructed in the model where it was determined that flow conditions at the dam toe would be affected. Different size rock protective schemes were then investigated for the overtopping impact area at the dam toe. Either quarried or precast blocks could be used for the large material. A potential source of quarried limestone was identified by geologists. Tests were run in the model using aluminum or concrete cubes representing 5-, 2-, and 1-ton blocks. Discussion with geologists indicated that a cubic shape would be representative of how the limestone would quarry. As noted, the model does not correctly represent jet breakup and air entrainment and consequently, evaluation of block stability in the model will be conservative. If the blocks are displaced in the model, they may or may not be displaced in the prototype.

The blocks should be placed directly on the bed rock. Use of bedding material would require use of a filter. Failure of the filter and local loss of the bedding material would cause failure of the protective blanket. It was also noted that with a placed or dumped blanket of large blocks, substantial venting would occur between blocks which would minimize the development of uplift pressures. Thus, the drains required with a reinforced concrete blanket would not be needed. A blanket of blocks two layers deep should be adequate.

Initially, 5-ton blocks were tested, represented by 4 ft cubes. They were modeled in concrete which has a specific weight of about 140 lbs/ft^3 which is less than the 165 lbs/ft^3 specific weight of limestone. The blocks were placed in a two-deep blanket. The blanket extended 25 to 50 ft downstream of the observed downstream limit of the impact zone and approximately 125 ft downstream from the powerplant. Both at discharges of 400,000 ft^3/s and 459,000 ft^3/s, displacement of top layer blocks occurred in the last 25 ft of the blanket. The nearest displacement to the dam was about 50 ft downstream and to the right of the base of the left buttress. The bottom layer was undisturbed with all flow conditions. Thus, the indications are that this blanket would adequately protect the dam foundation. Further review of the quarried rock source indicated that blocks as large as 5 tons probably could not be quarried. As a result, 2-ton and 1-ton blocks were also tested. Both of these were tested using aluminum blocks which correctly represent the limestone specific weight. Blocks were placed both in a uniform grid and in a somewhat random dumping (although because the blocks were cubes they tended to nest together in a fairly organized way). As with the 5-ton blocks, there was displacement in the top layer of the 2-ton blocks. Again, the displacement was about 50 ft downstream and somewhat to the right of the base of the left buttress. At 400,000 ft^3/s, the displacement was only minor. At 459,000 ft^3/s, there was substantial scour of downstream fill represented by 12- to 42-in

angular material with displacement of top layer blocks (fig. 21). Again, this displacement was well away from the structure and the bottom layer was not disturbed. Thus, it was felt that the 2-ton blocks supplied good foundation protection. Tests with 1-ton blocks showed about the same result with additional erosion of downstream fill to the fixed bed of the model on the left and right sides.

The model results were discussed with the design team. The relative difference in performance between the 1- and 2-ton rock blocks was minimal. The availability of rock sizes was determined and the gradation for the rock protection decided. The final design consisted of graded stones with weights between 1000 to 4450 lbs., with 75 percent between 2200 to 4450 lbs. The stones were placed in a 7-ft-thick layer for about 150 ft downstream from the dam and about 4 ft thick for the next 75 ft downstream.

Chute Cavitation and Aerator Design - The cavitation and aeration ramp computer models developed by Falvey [3] were run for each spillway chute with individual spillway discharges ranging from 5,000 ft^3/s to 50,000 ft^3/s. The computer models cannot evaluate the influence of superelevation, horizontal curves, or non-uniform flow distribution. Therefore, initial flow conditions were set for the computer model at the top of the 60-ft-wide chute sections based on velocity and water depth profile data taken from the model.

The cavitation potential for the spillway chutes was first determined. The cavitation potential is defined by a flow sigma based upon the flow velocity. Runs of the cavitation program predicted flow sigmas as low as 0.23 on the lower chutes. Lowest sigmas occurred at discharges of 20,000 to 30,000 ft^3/s on each chute. These runs predict that unless good surface tolerances can be maintained, that a potential for significant cavitation damage exists. Tolerances required are no abrupt offsets greater than 0.25 in and no chamfers steeper than 1 on 16. It seemed unlikely that flow surfaces of this quality would be maintained over the life of the structure. Ensuring air near the chute inverts will reduce cavitation potential. Significant free surface air entrainment occurs high on both chutes due to the rough flow conditions. This may yield residual entrained air in the potential high cavitation zones at the lower ends of the chutes, although it is difficult to quantify. Because of uncertainties about future flow surface conditions and available entrained air, this evaluation indicated that it would be prudent to install aeration ramps.

Initially, the designers requested an aerator design with installation of air vents on only one side of the chute, so that substantial excavation for vents on the uphill sides of the chutes would not be required. Initial output from the computer program indicated that relatively large ramps with offsets away from the flow about 2 ft high were required to obtain sufficient air passage area under the flow. A ramp with a 2-ft offset on the existing chutes would generate considerably more air entrainment than is required for cavitation damage control. The heavy air entrainment predicted could cause problems with flow bulking and containment of the flow in the chute. In addition, for these large ramps with their high air demand, very large vents with cross sections in excess of 50 ft^2 would have to be included to maintain acceptable air velocities.

Further analysis indicated that a ramp with a 4-in offset and with a ramp angle of 2 degrees to the chute surface would entrain about 10 percent air (percentage of the water discharge). The ramps should be located at about elevation 2420 to ensure no tailwater influences. This is more than a sufficient quantity of air to control cavitation damage on both the left and right spillways. The analysis indicated that an air vent on one side of the chute with a 16 ft^2 cross section would be adequate to supply required air flow rates and maintain acceptable air flow velocities. The air flow passage under the deflected water or the duct which transports air to the underside of the flow should also have about a 16-ft^2 cross section. The 4-in ramp does not provide sufficient area and an alternative slot design such as the "duct under ramp" or "duct downstream of ramp" would be required (fig. 22). Both designs include a duct that is below the chute grade and both ducts have a potential for collecting water and debris. Provisions for duct drainage sufficient to handle gate leakage should be included in the design.

Alternative aeration slot designs were then considered to develop a design that was easier to construct. A design was needed that omitted free-standing air vent towers and significant excavation into the existing spillway inverts and would not accumulate debris.

Therefore, an aerator with ramps on the spillway face and side walls was designed. The previous ramp with a 4-in offset on the spillway invert will entrain sufficient quantities of air to protect against cavitation damage. However, without modifying the spillway invert, there is inadequate air passage under the flow to yield acceptable aeration. By supplying air from both sides of the chute, the air flow discharge in each vent is halved, reducing the required area of each. An air vent cross section of 4.5 ft^2 was found to be adequate, realizing that for very rare high spillway flows air vent velocities would be up to 300 ft/s. This cross section can be achieved across the chute invert by excluding the new concrete overlay for about 3 ft below the ramp lip (fig. 23). The transition back to the full 9-in overlay should be gradual to supply additional vent cross section and to reduce the angle in the potential impingement area. Impingement on the transition would occur during low discharges. The 13 degree angle is representative of the transition that should be considered.

Flow trajectories from the ramp lip to the downstream impingement with the chute face were computed for a range of discharges both with and without spillway gate control. The computed trajectories show no flow impingement until the flow is well past the aeration slot. This is the case for discharges as low as 2,000 ft^3/s. This indicates that flow impingement on the slot will occur only at small discharges for which cavitation potentials are low and air entrainment on the upper chute is high. Therefore, the slots as proposed should not be a source of additional cavitation.

Observation of the side wall ramps in the model show that a 1-ft offset on the outside walls of both chutes creates an excessive flow separation with potential finning above the top of the chute wall. However, the 1-ft offset was satisfactory on the inside walls of both chutes. Thus, it is recommended that the final design include an 8-in offset over 10 ft on the outside walls and a 1-ft offset over 10 feet on the inside walls (fig. 23). Observations in the physical model show that the aeration slots will yield adequate venting over the full discharge range.

Unbalanced Gate Operation - A series of tests were run to identify optimum and worst case unbalanced gate operations. Unbalanced gate operation includes those operations for which all gates are not open uniformly. First, it is recommended, even with unbalanced gate operation, that the spillways be operated with each spillway passing about half of the total spill. The flows exiting from the two spillways tend to offset one another, yielding a mid-channel flow directed downstream. Use of only one spillway will cause an unbalanced flow which crosses the river channel and will scour the opposite bank. The need for balanced discharge distribution between spillways increases with discharge and is recommended for any discharge greater than 5,000 ft^3/s.

A wide range of operating gate combinations was observed for combined spillway discharges ranging from 4,127 ft^3/s to 38,600 ft^3/s. All six gates from both spillways were used for the testing. The gates were numbered 1-6 from left to right. Unbalanced gate operation was studied with 2-ft increments in gate openings. All tests were run with the reservoir water surface at the top of the closed gates, about elevation 2523. With combined spillway releases above about 40,000 ft^3/s, balanced gate operation with all six gates is recommended. Unbalanced gate operation can be used to minimize standing waves, flow impingement on chute walls, and finning. However, if the structure is improperly operated, unbalanced gate operation can aggravate poor flow conditions.

Flow conditions on the right spillway chute are strongly influenced by the superelevation in the upper chute. Flow released through the outside gate is strongly concentrated and redirected to the inside by the superelevation, impinging severely against the left chute wall. Flow from the inside gate, however, needs to be turned through a greater angle and works well with the superelevation. Use of the inside or inside and middle gates significantly reduces the standing wave impingement against the left wall. This operation results in a uniform flow distribution on the lower chute compared to the poor distribution observed with balanced operation. Thus, recommended unbalanced gate operation for the right spillway typically suggests greater flows through the inside or inside and middle gates.

On the left spillway, the observed standing wave is more a function of the flat upper chute gradient and the horizontal curve. The standing wave is increased by use of the inside gate and the angle through which the flow must turn. Use of the outside and middle gates reduces the turn angle which reduces the standing wave and improves the flow distribution on the lower chute and is the recommended unbalanced operation for the left spillway. A summary of the tested unbalanced gate operations are outlined in Table 2 and should function as a guide, requiring interpolation for variations in discharge and reservoir elevation.

Table 2. - Observations of unbalanced gate operation. Gates numbered 1-6 from left to right looking downstream.

Rating	Discharge (ft^3/s)	Gate Opening (ft)					
		Left Spillway			Right Spillway		
		Gate No.1	Gate No. 2	Gate No. 3	Gate No. 4	Gate No. 5	Gate No. 6
Optimum	8,250	4	0	0	4	0	0
Optimum		2	2	0	2	2	0
Worst		0	0	4	0	0	4
Worst		0	2	2	0	2	2
Optimum	16,500	10	0	0	10	0	0
Optimum		8	2	0	8	2	0
Worst		0	0	10	0	0	10
Worst		0	4	6	0	2	8
Optimum	25,000	4	4	4	10	2	2
Optimum		10	0	6	10	2	2
Worst		0	6	10	0	4	10
Optimum	35,000	6	8	8	10	10	2
Worst		2	10	10	2	10	10
Optimum	38,600	8	8	8	12	12	4
Optimum		10	10	6	12	12	4
Worst		4	12	12	4	12	12

References

1. Randle, T. J., "Tailwater Study for Coolidge Dam, San Carlos Irrigation Project, Arizona, Bureau of Indian Affairs," Memorandum to Head, Sedimentation and River Hydraulics Section, Bureau of Reclamation, August 7, 1984.

2. Ervine, D. A., and H. T. Falvey, "Behavior of Turbulent Water Jets in the Atmosphere and in Plunge Pools," *Proceedings of the Institution of Civil Engineers*, Part 2, Vol. 83, pp. 295-314, March 1987.

3. Falvey, H. T., "Cavitation in Chutes and Spillways," U.S. Bureau of Reclamation Engineering Monograph No. 42, April 1990.

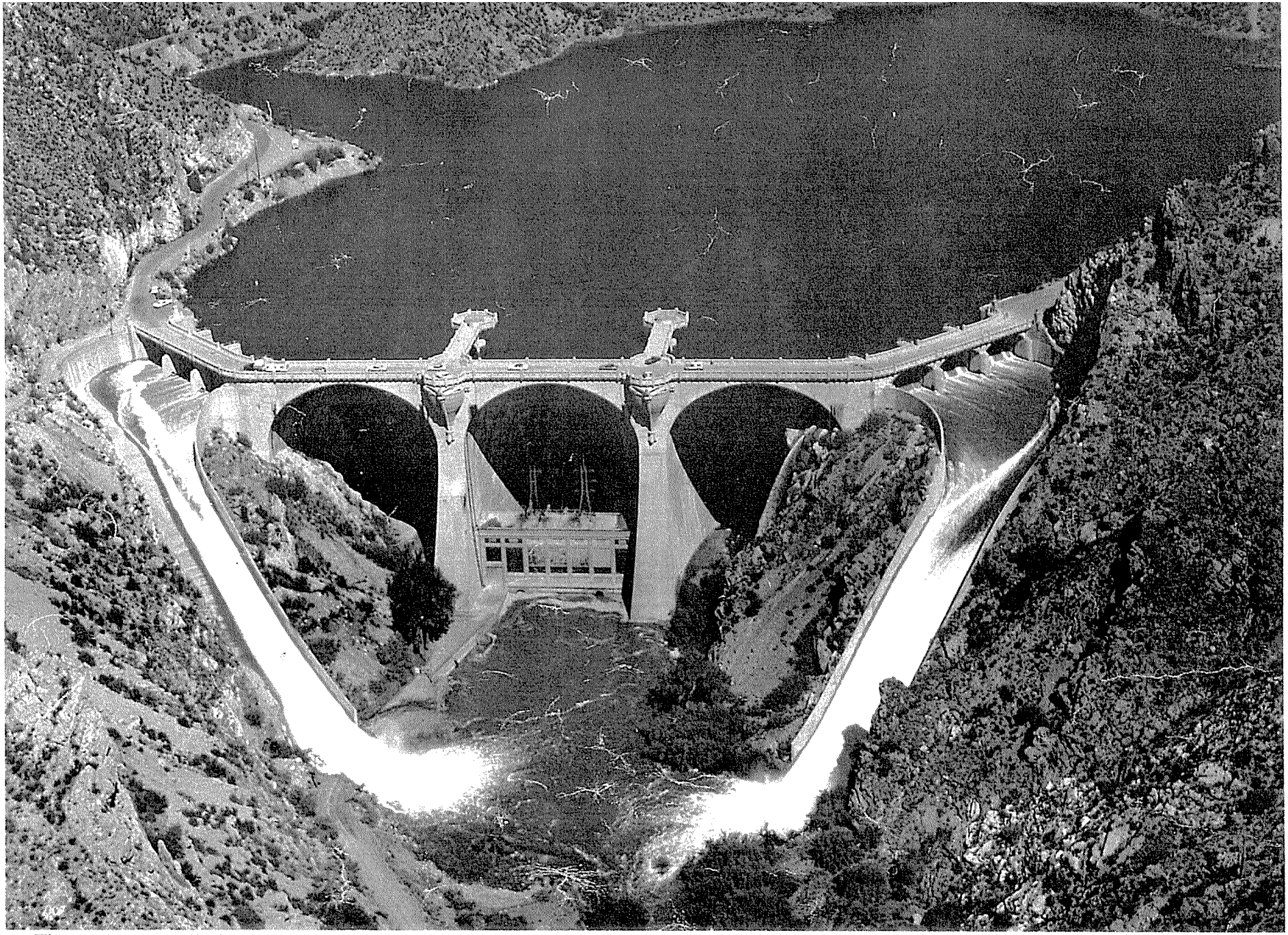

Figure 1 - Overall view of Coolidge Dam, Arizona.

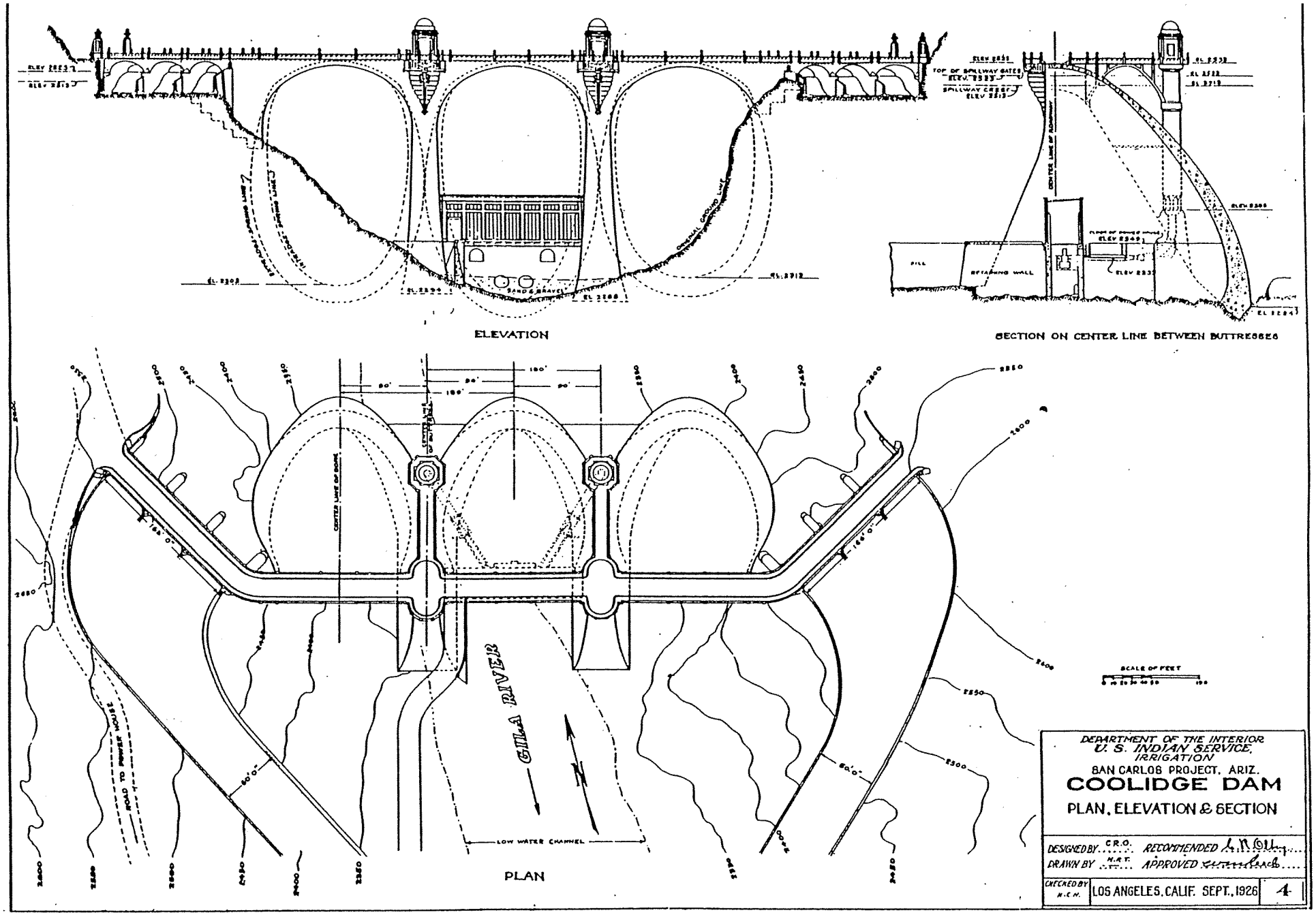

Figure 2 - Plan, elevation, and section of existing dam.

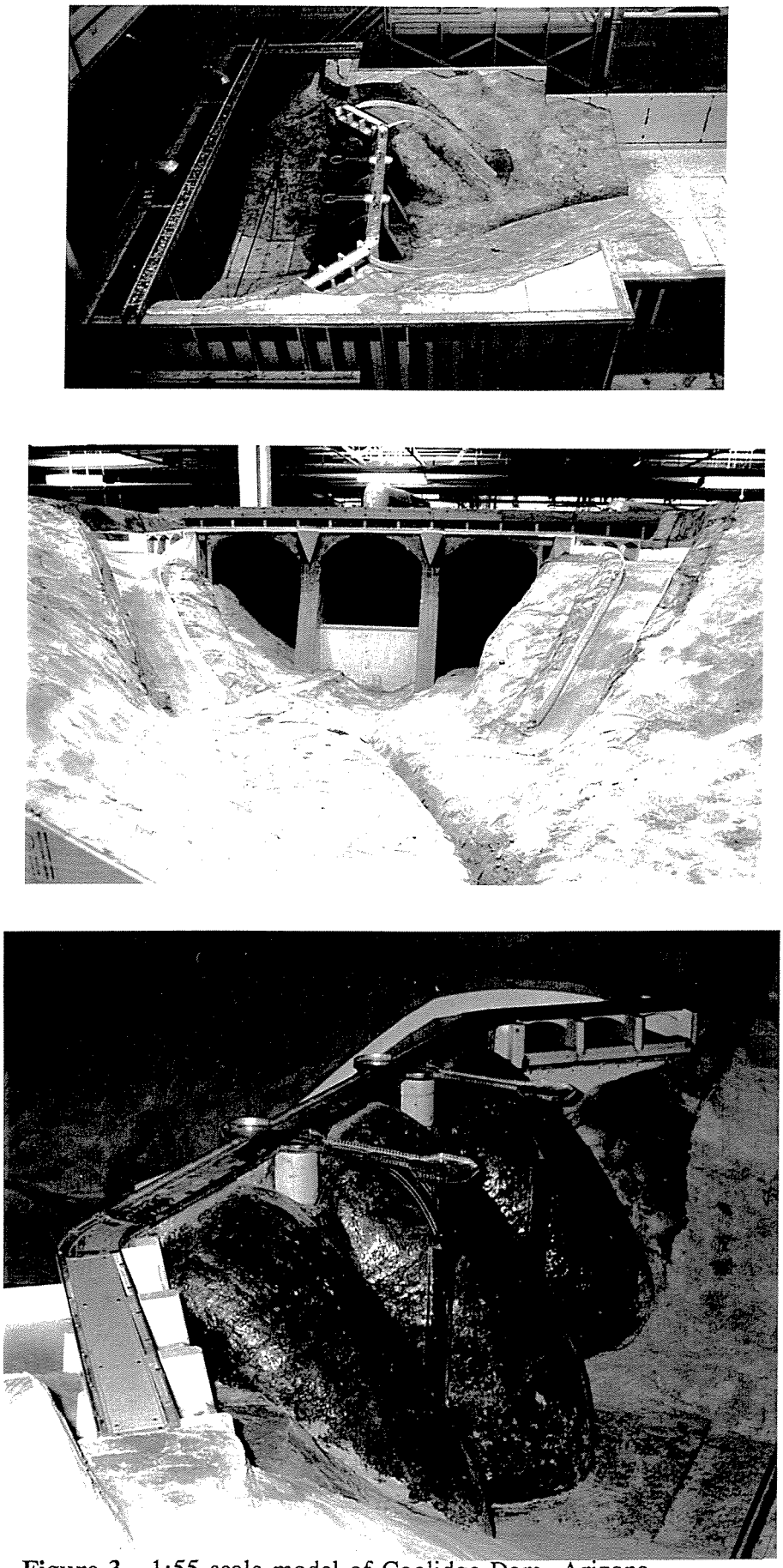

Figure 3 - 1:55 scale model of Coolidge Dam, Arizona.

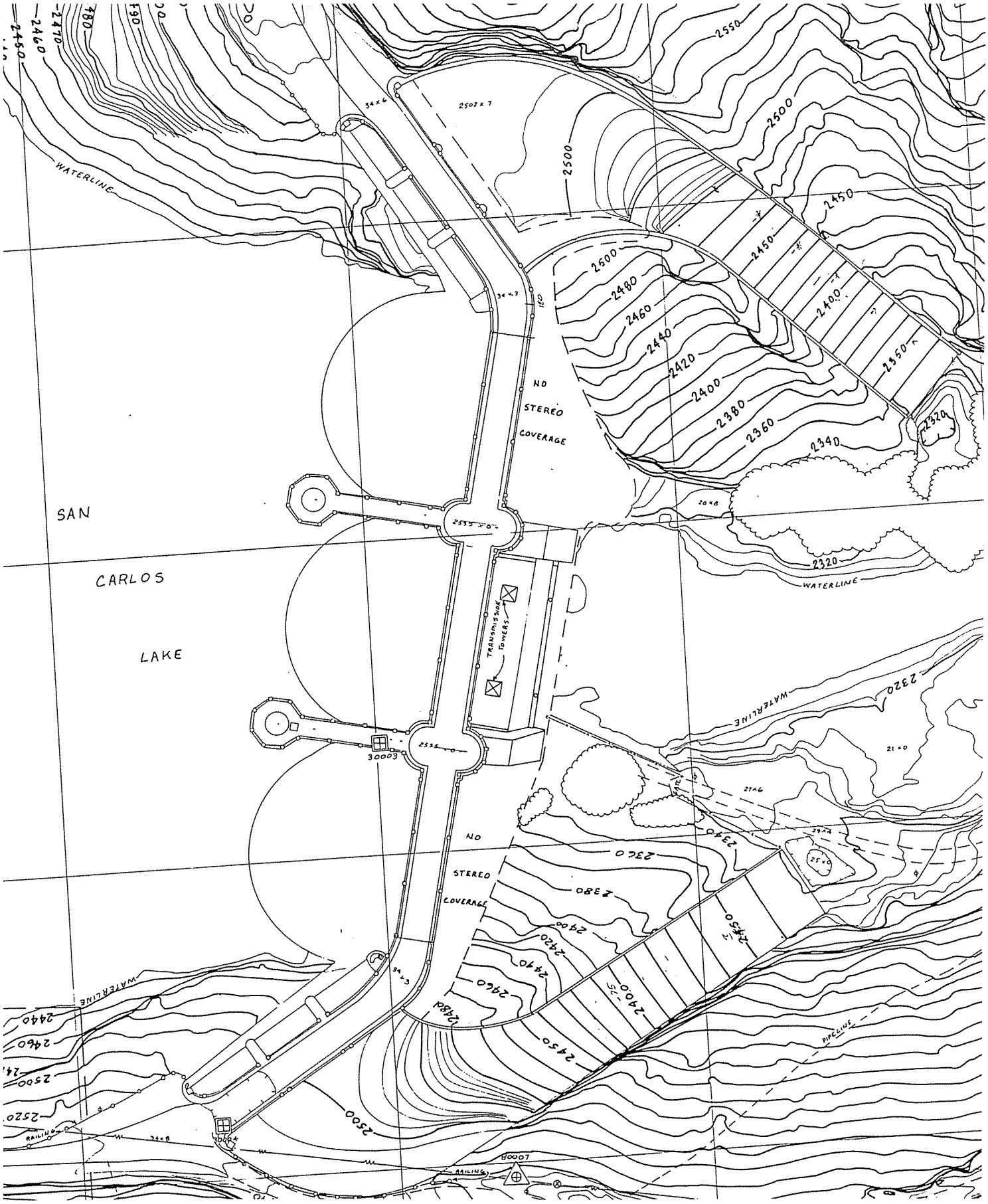

Figure 4 - Topographic map showing contours of the spillway chutes.

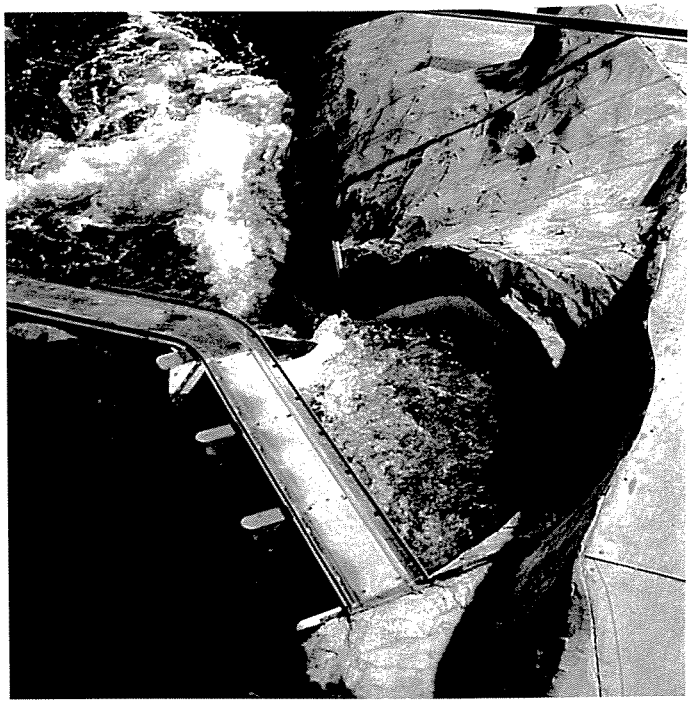

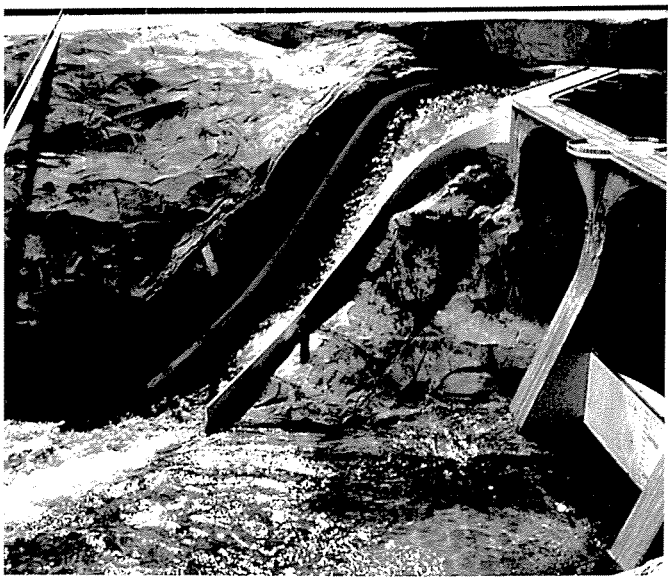

Figure 5 - Right spillway flows with a combined spillway release of 75,000 ft^3/s.

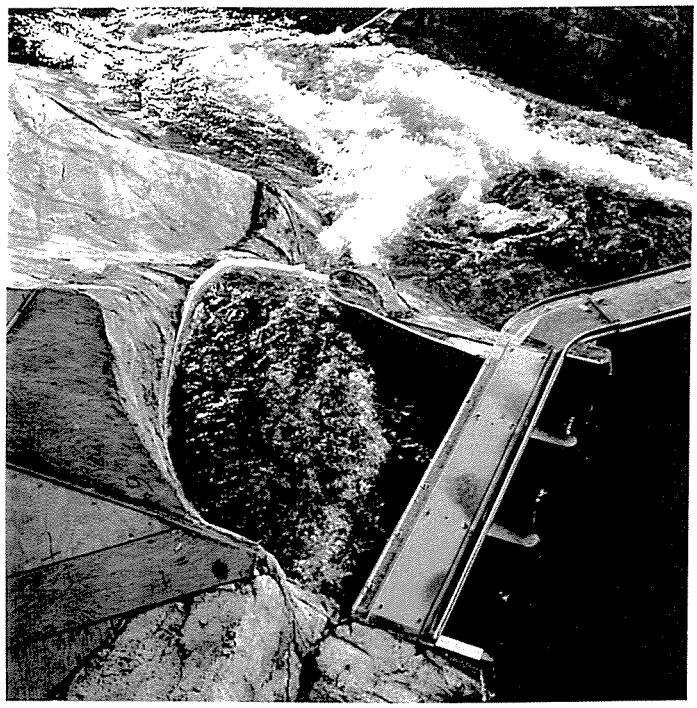

Figure 6 - Left spillway flows with a combined spillway release of 75,000 ft^3/s.

Figure 7a - Combined spillway flows of 200,000 ft^3/s showing the left spillway and the beginning of overtopping flows.

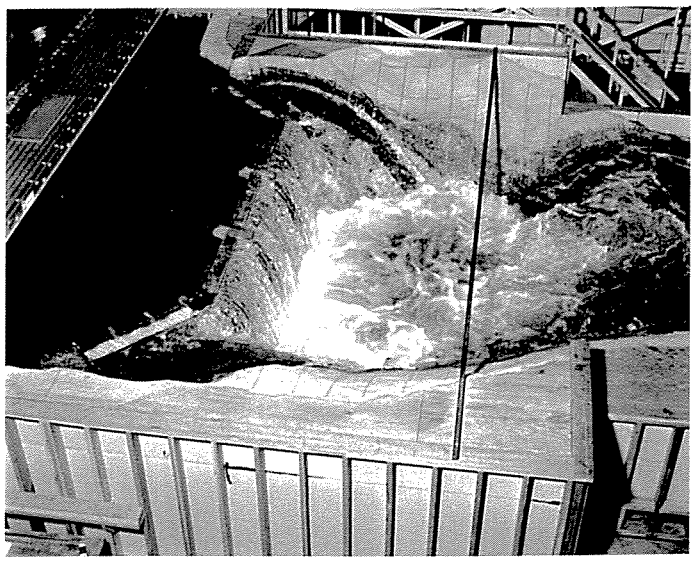

Figure 7b - Combined spillway flows of 459,000 ft^3/s showing the left spillway and dam overtopping.

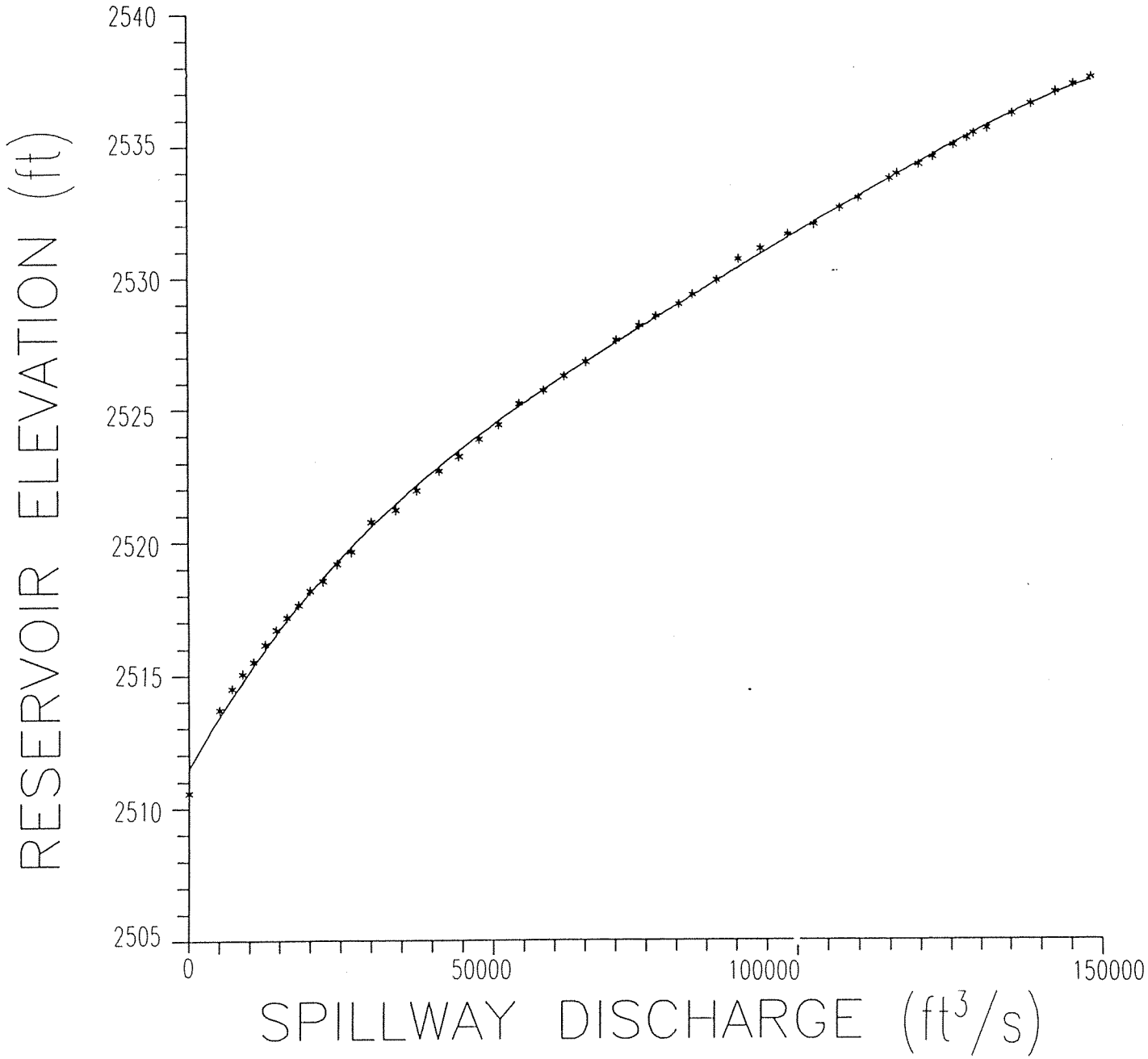

Figure 8 - Combined spillway discharge rating curve for the ungated existing spillways.

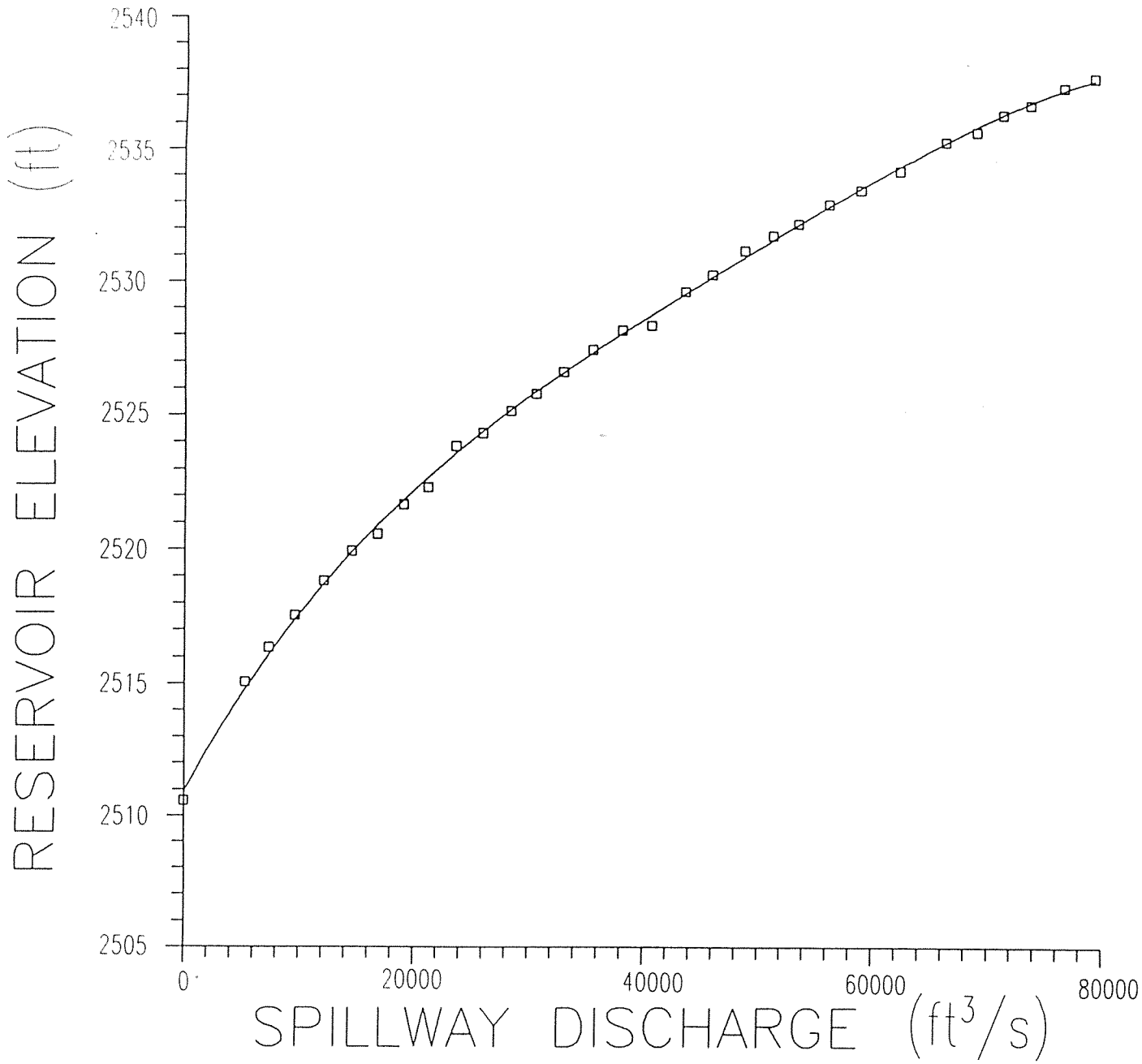

Figure 9 - Right spillway discharge rating curve for the ungated existing spillway.

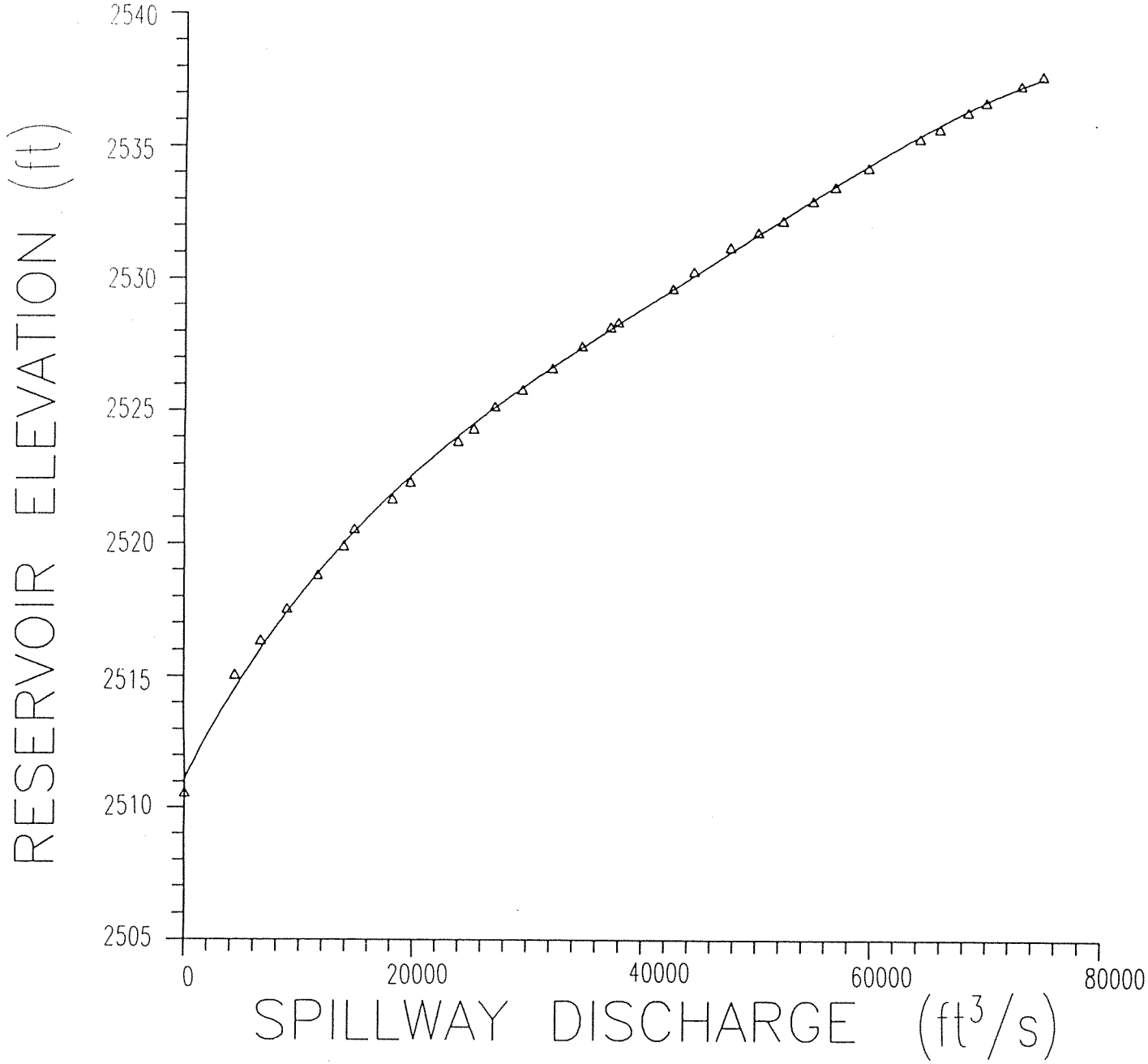

Figure 10 - Left spillway discharge rating curve for the ungated existing spillway.

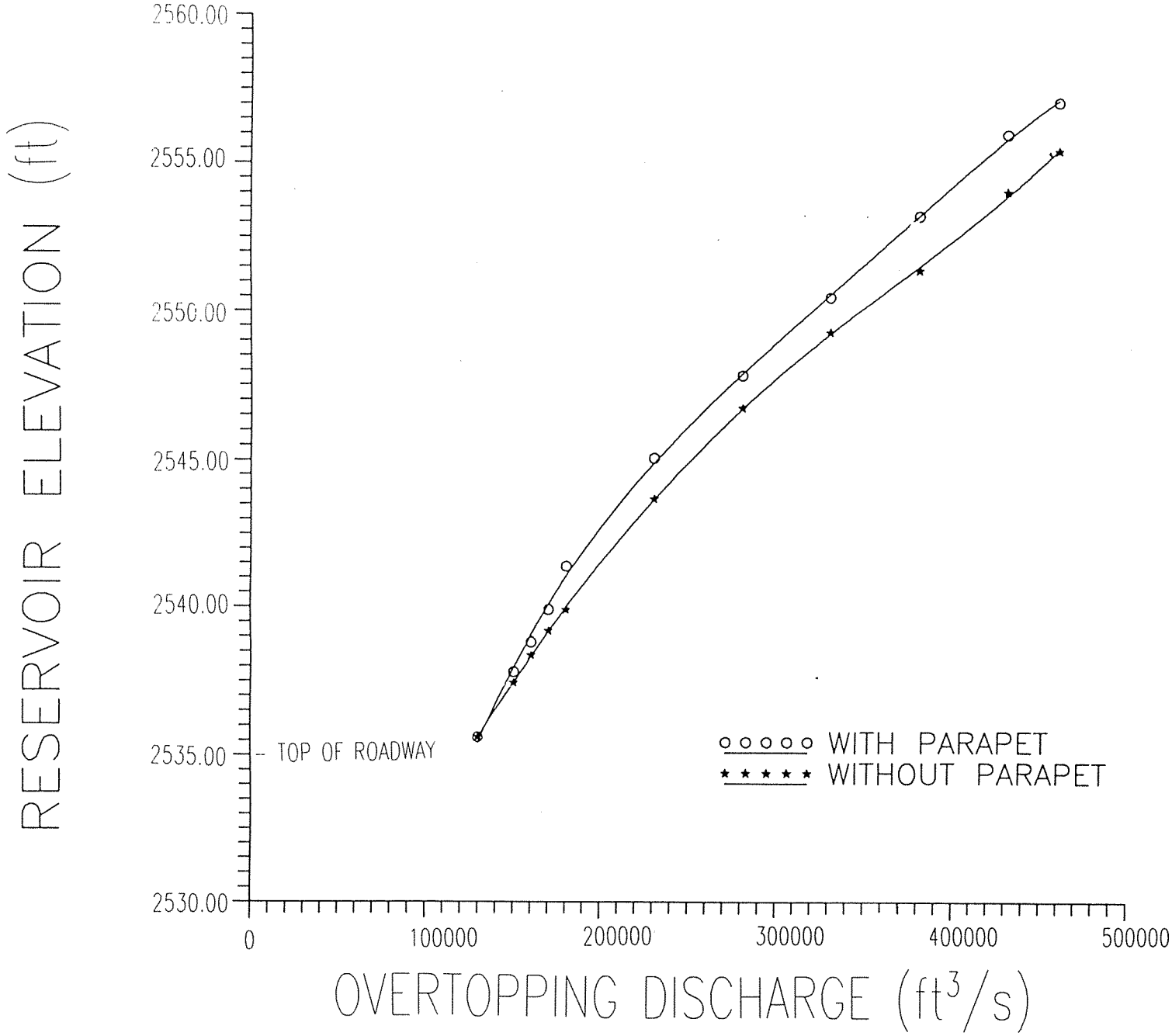

Figure 11 - Discharge rating curves for flow over the dam, with and without the roadway parapet.

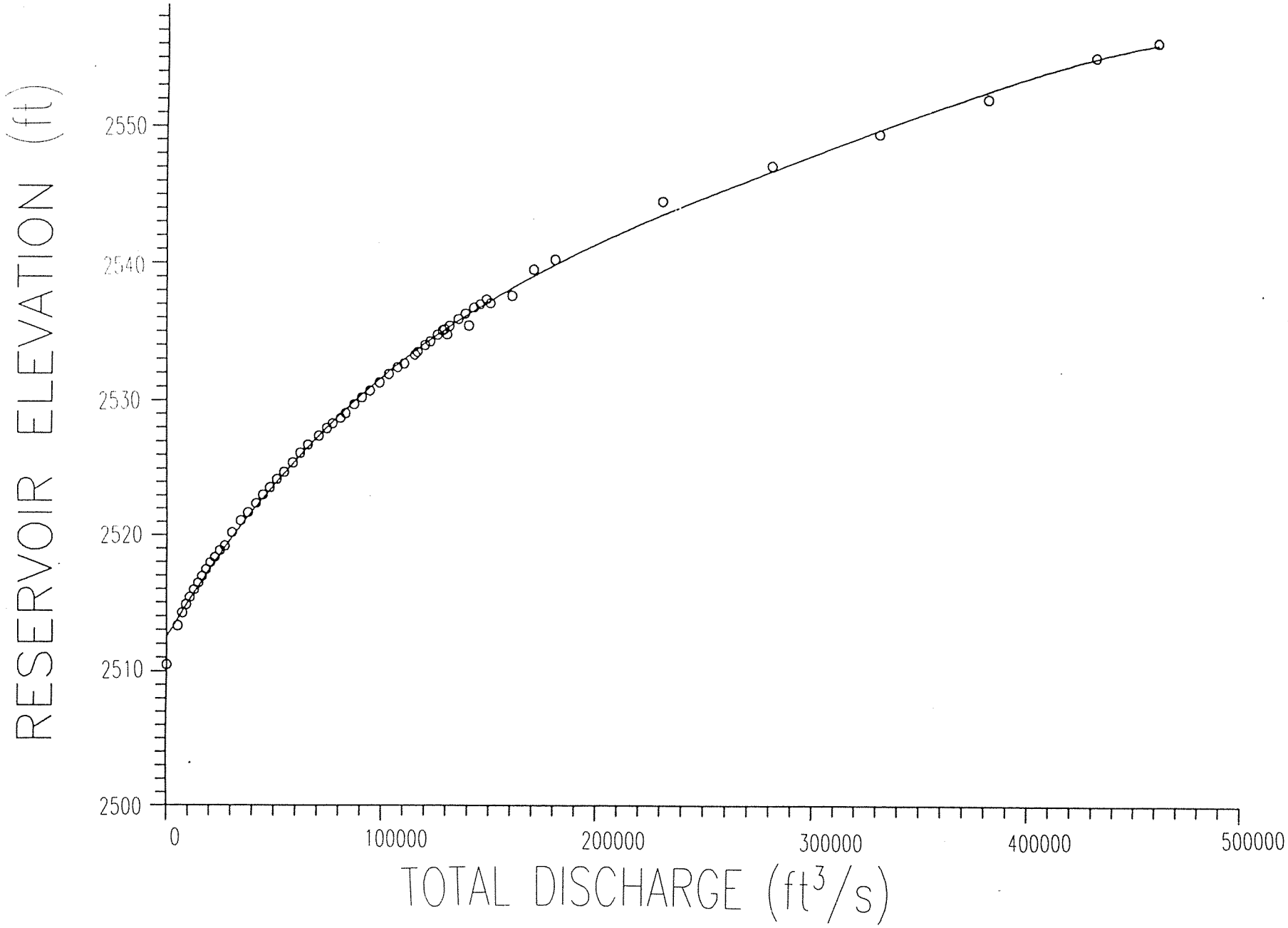

Figure 12 - Total discharge rating curve for ungated spillways and dam overtopping with the roadway parapet walls.

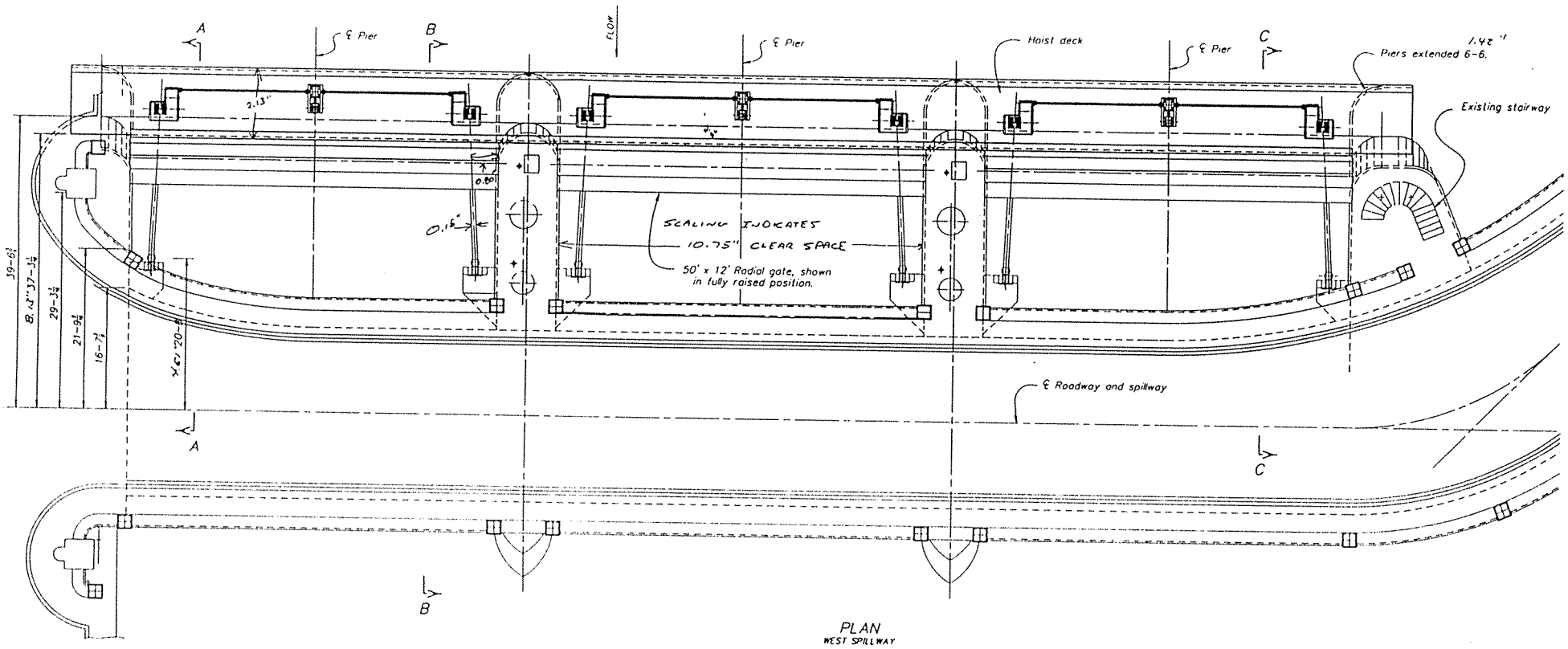

Figure 13 - Modified pier design for radial gate installation.

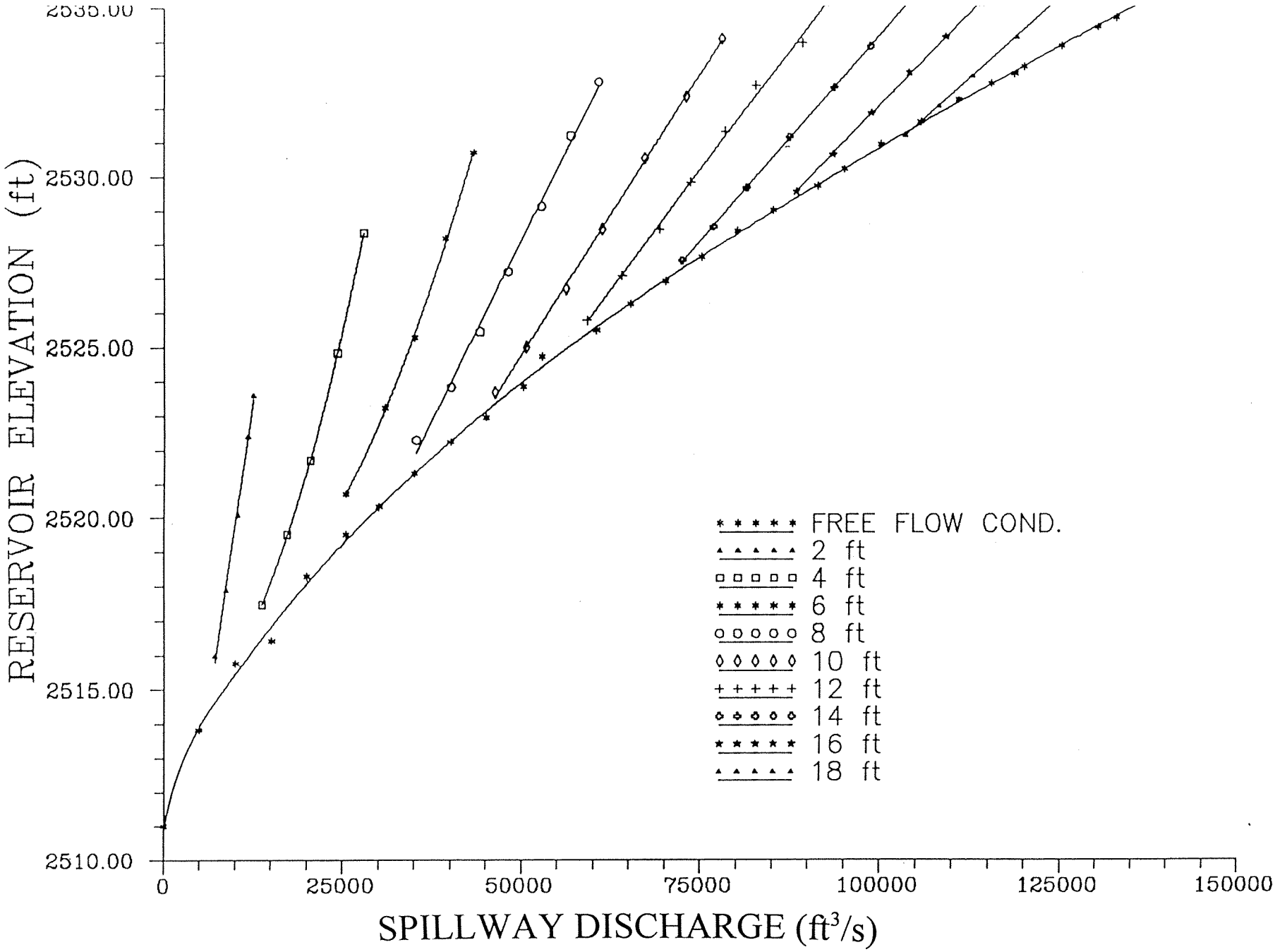

Figure 14 - Combined spillway discharge rating curve for modified crest and piers with 6 radial gates controlling the flow.

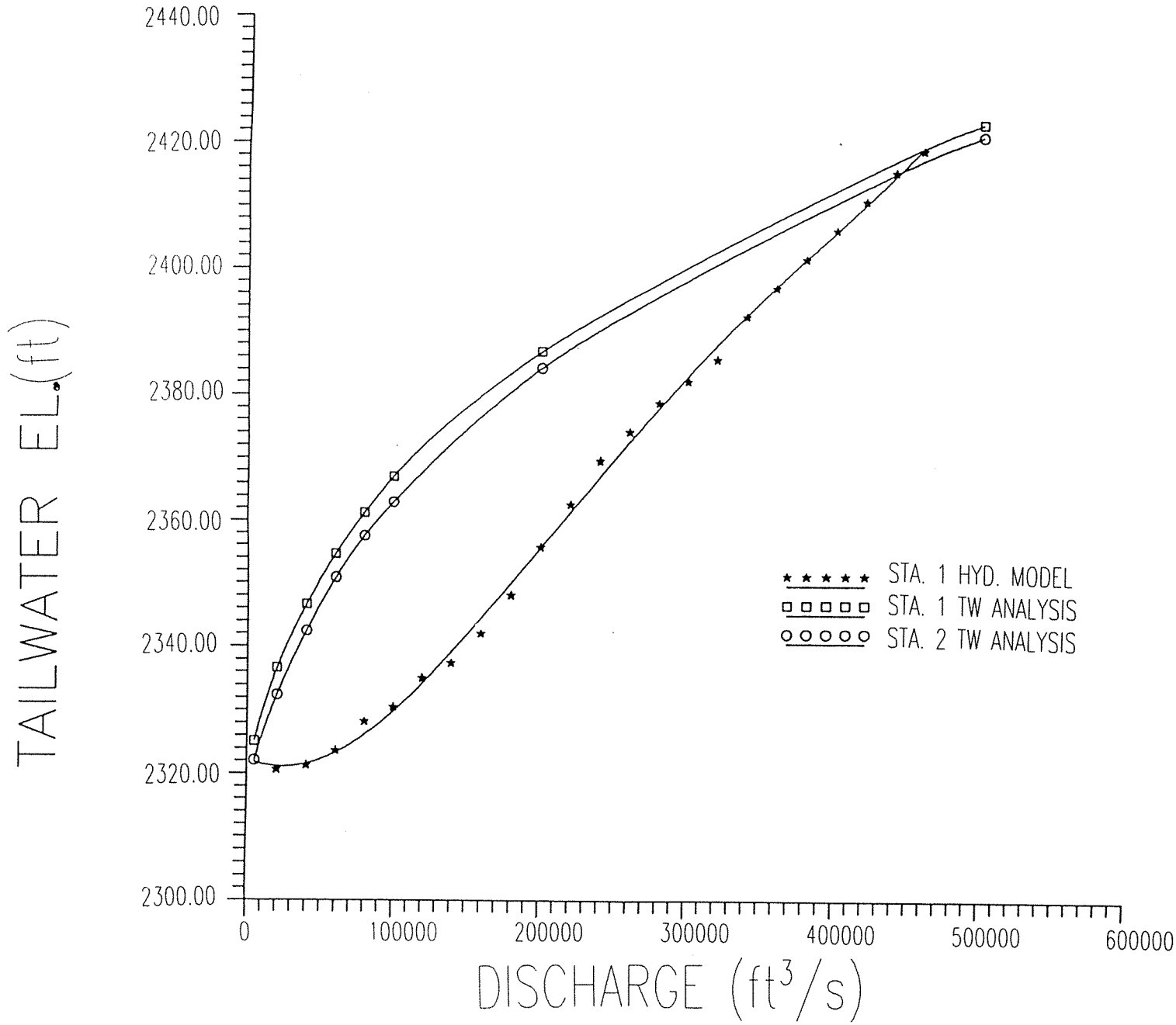

Figure 15 - Tailwater rating curves near the toe of the dam, both at station 1 and 600 ft downstream, station 2.

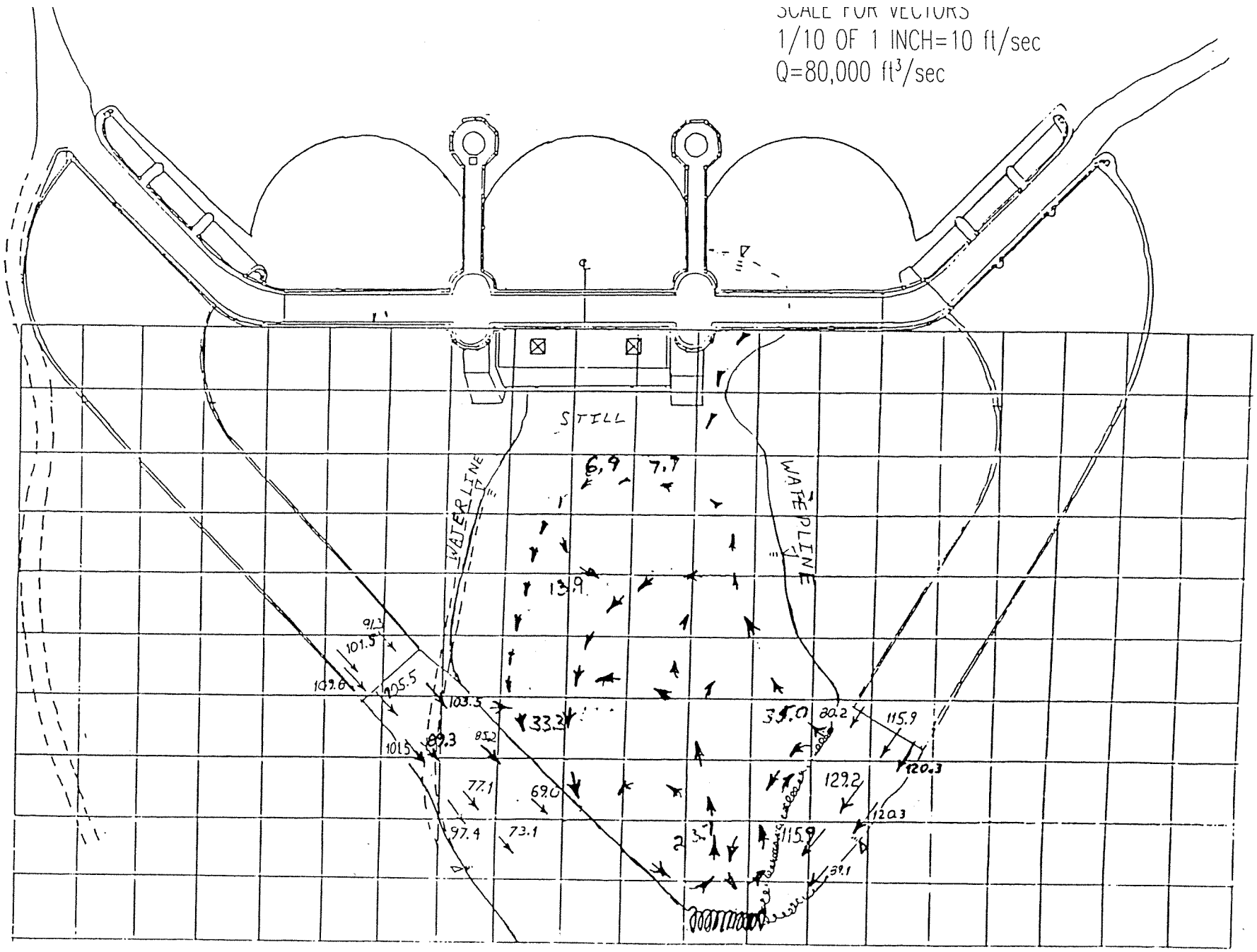

Figure 16 - Video recorded flow velocities at the end of the chutes and in the river channel from a discharge of 80,000 ft³/s.

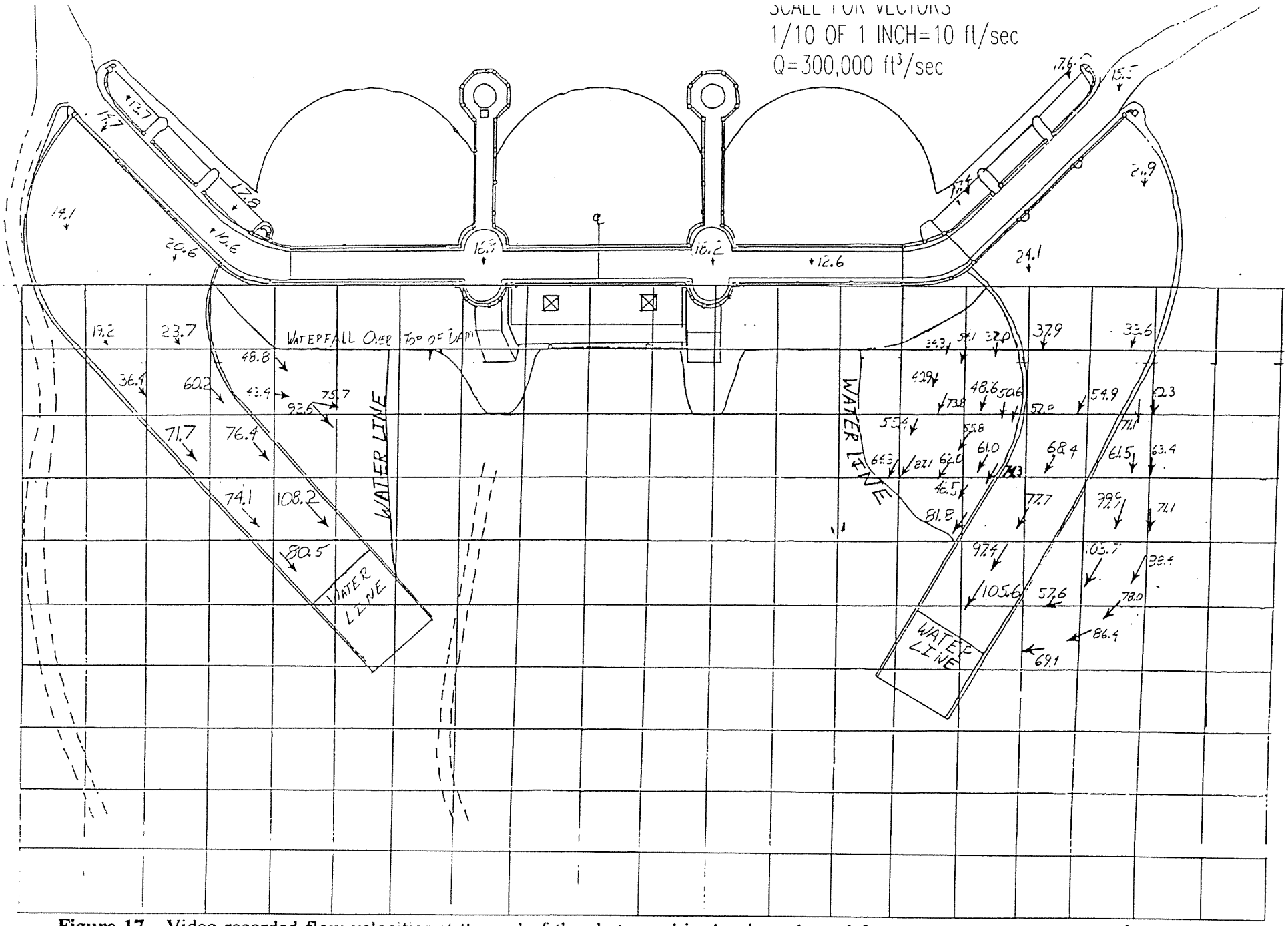

Figure 17 - Video recorded flow velocities at the end of the chutes and in the river channel from a discharge of 300,000 ft³/s

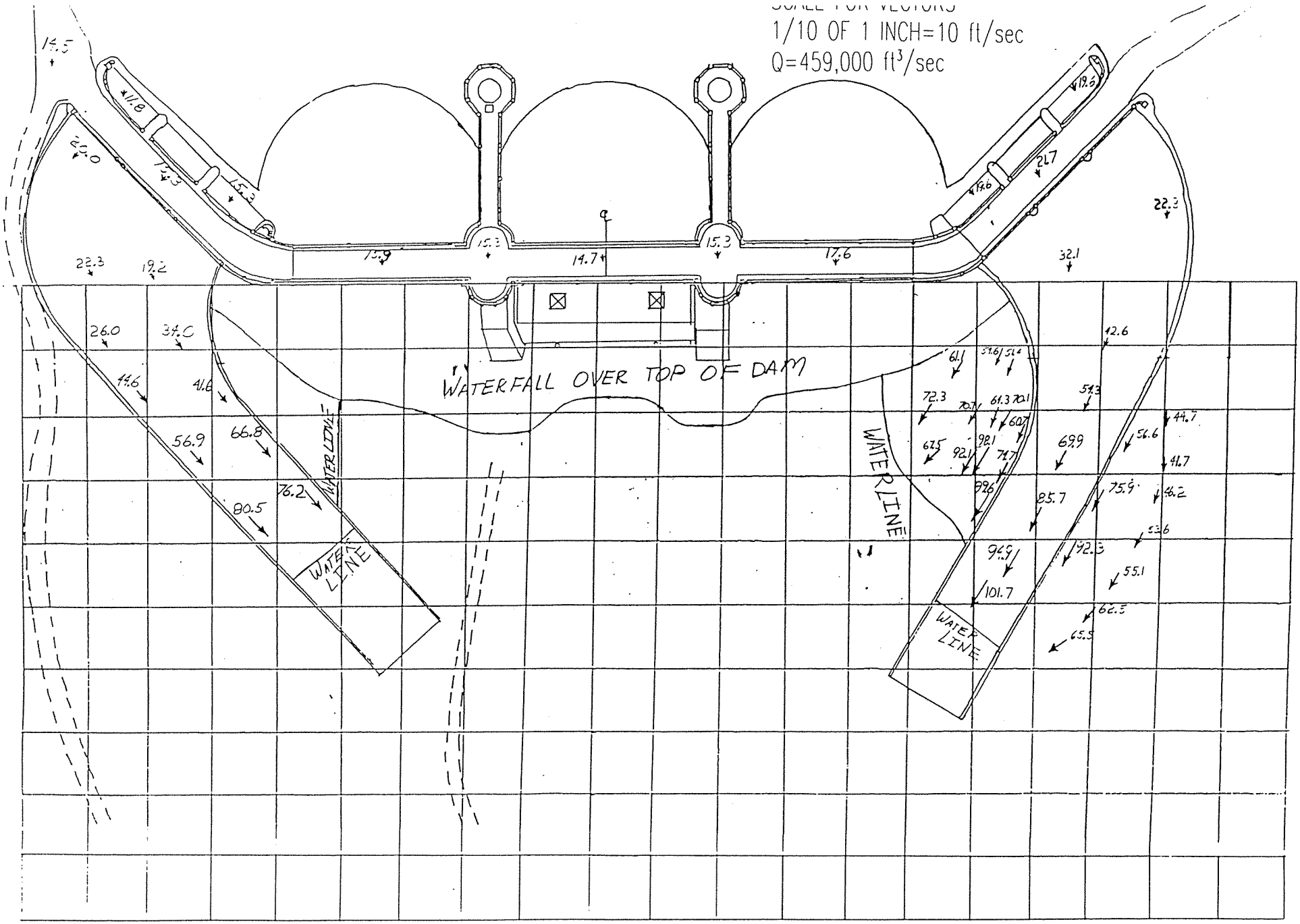

Figure 18 - Video recorded flow velocities at the end of the chutes and in the river channel from a discharge of 459,000 ft³/s.

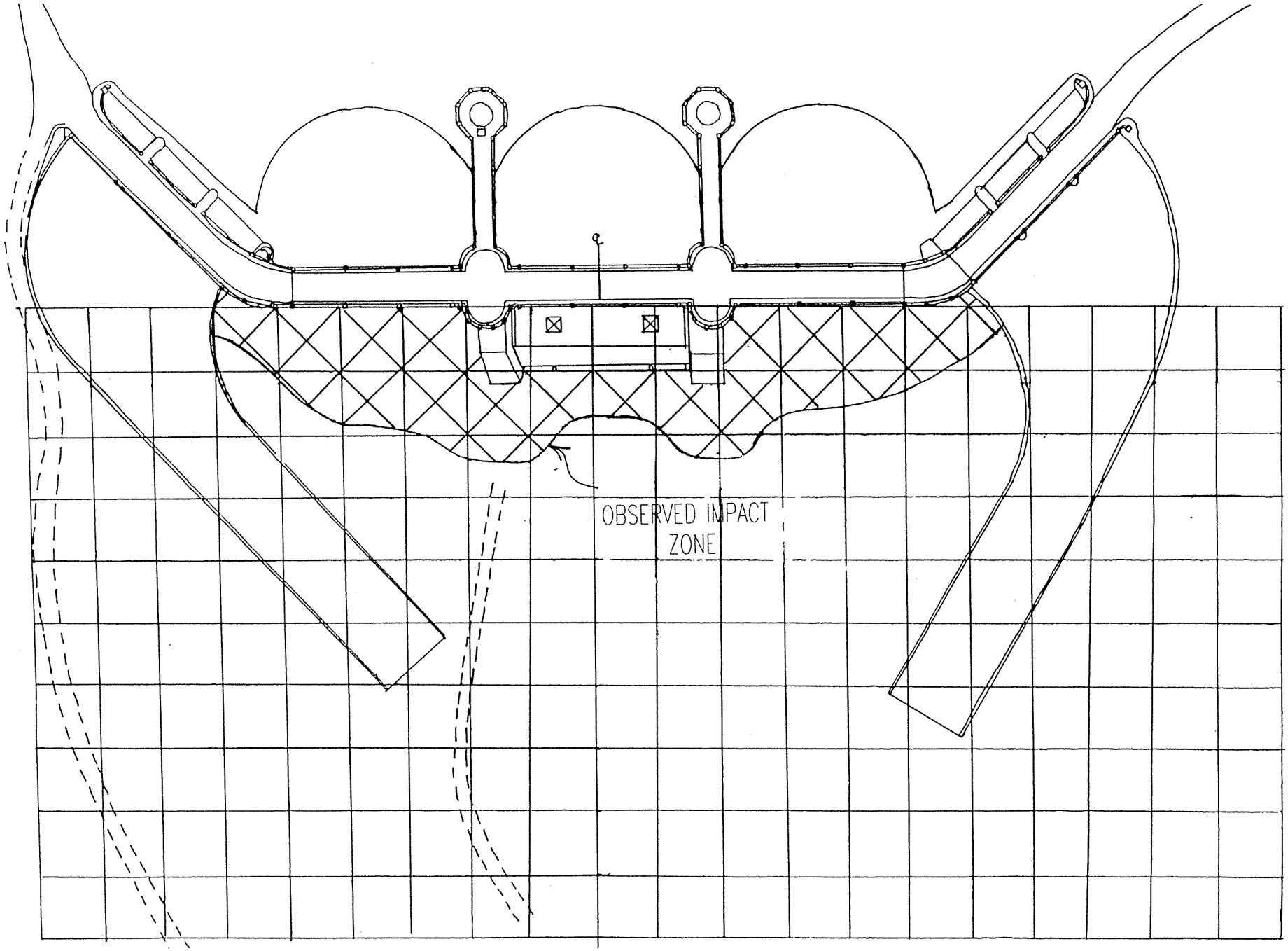

Figure 19 - Observed impact zone for the full range of discharges (each grid = 50 ft).

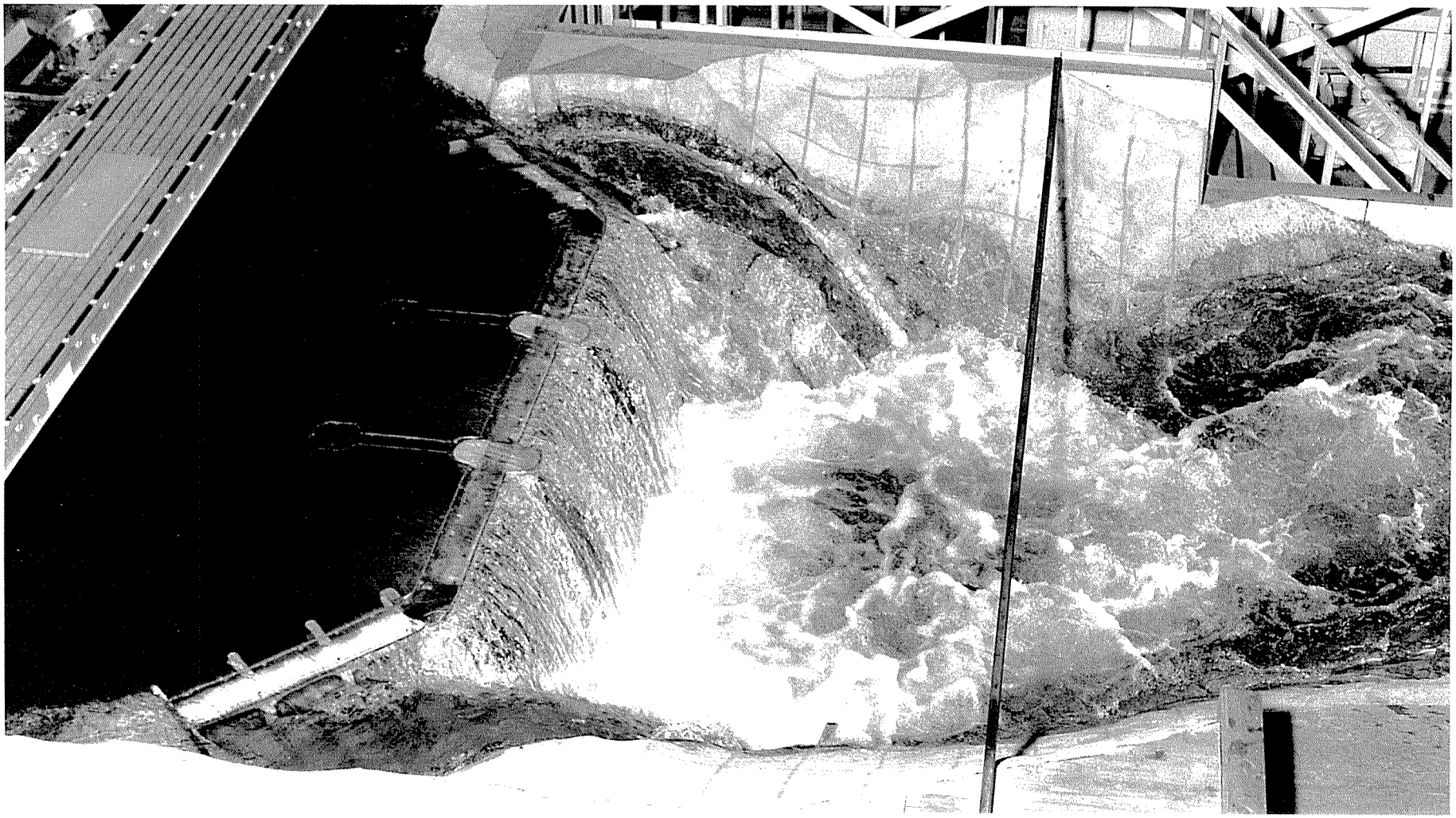

Figure 20 - PMF flow through spillways and over the dam showing the extent of required overtopping protection.

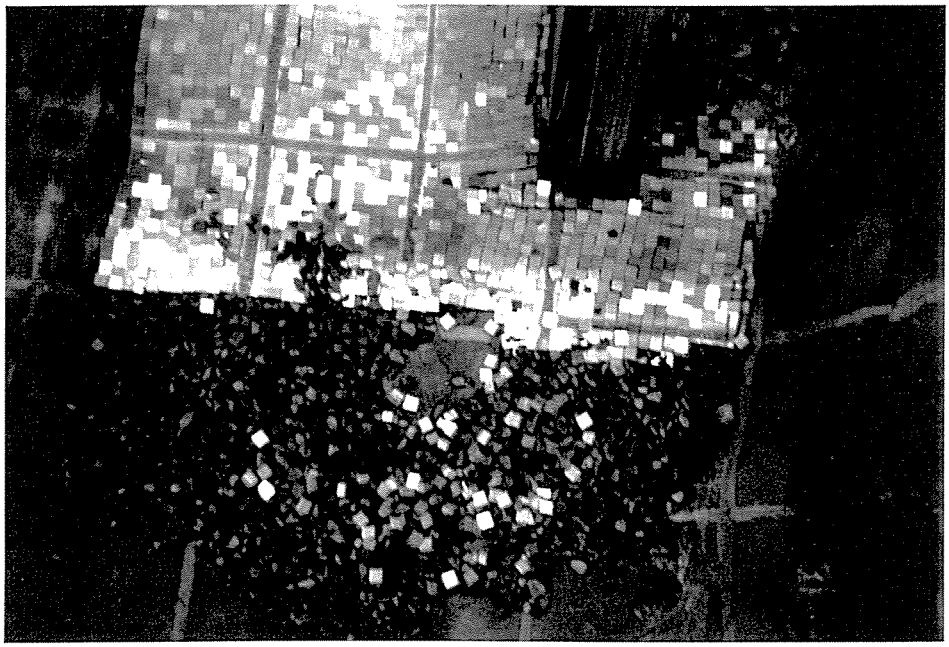

Figure 21 - Rock blocks placed at the toe of the dam to investigate acceptable erosion protection during overtopping. Block movement after the PMF is shown.

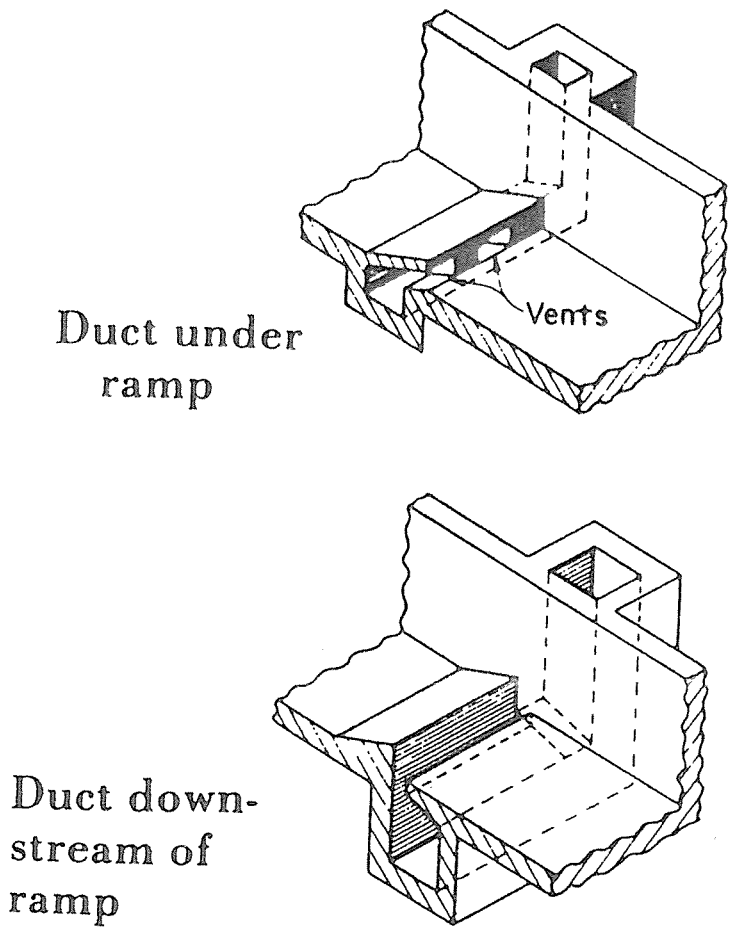

Figure 22 - Methods to supply air to aerators.

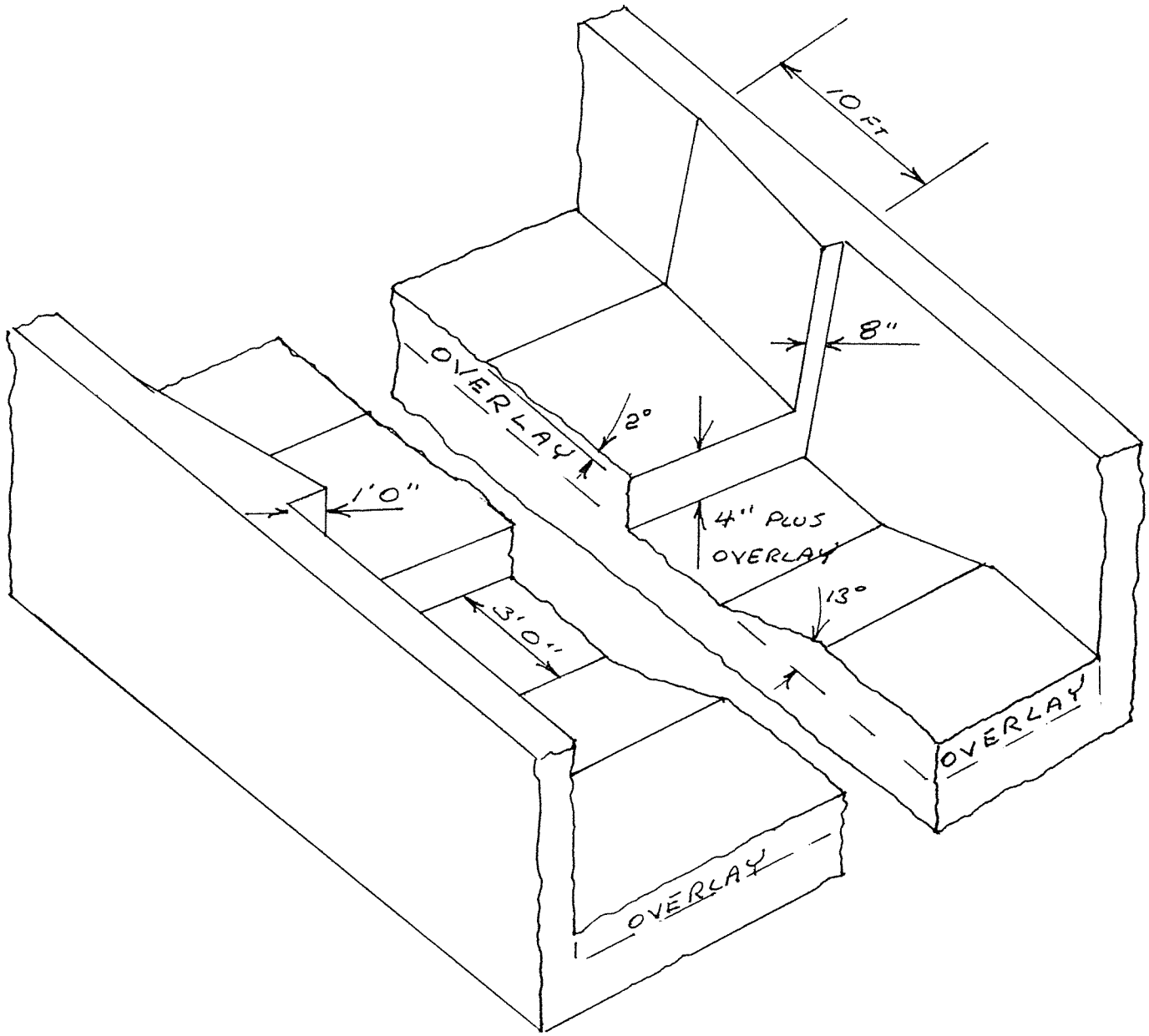

Figure 23 - Sketch of aeration slot for the left spillway. The right spillway slot will be a mirror image.